Proceedings of the

3rd Oxford Tidal Energy Workshop

7-8 April 2014, Oxford, UK

Proceedings of the 3rd Oxford Tidal Energy Workshop (OTE 2014)

7-8 April 2014, Oxford, UK

Monday 7th April

Tuesday 8th April

Session 5: Farm Scale Problems

Chair: Takafumi Nishino (University of Oxford)

Poster Presentations (2)

Session 6: Device Scale Problems (2)

Chair: Tim Stallard (University of Manchester)

Workshop Organisers:

Richard H. J. Willden (Chairman) University of Oxford
Takafumi Nishino (Co-Chairman) University of Oxford (moving to Cranfield University in May 2014)

Scientific Committee Members:

T. A. A. Adcock (University of Oxford)
G. T. Houlsby (University of Oxford)
I. Masters (Swansea University)
T. Nishino (University of Oxford)
T. Stallard (University of Manchester)
P. K. Stansby (University of Manchester)
C. Stock-Williams (E.ON)
R. H. J. Willden (University of Oxford)

Sponsor: Oxford Martin School (University of Oxford)

Improving the cost-effectiveness of Darrieus hydrokinetic turbines

Brian Kirke
Barbara Hardy Institute, University of South Australia

Summary: Contrary to popular belief, Darrieus hydrokinetic turbines (HKTs) can be just as efficient as axial flow turbines. Their advantages include (i) straight untwisted blades which are relatively easy to construct, (ii) insensitivity to changes in flow direction, and (iii) rectangular swept area, facilitating close packing and ducting, which can increase power output from a given site. In their basic fixed pitch form they suffer from poor starting torque, low efficiency, shaking and torque ripple, but design improvements can eliminate or greatly reduce these disadvantages and greatly improve cost-effectiveness. This paper evaluates these options.

Introduction

It is widely believed that Darrieus hydrokinetic turbines (HKTs) are inherently less efficient than axial flow turbines, but this is not true. Two dimensional modelling by [1] of a Darrieus HKT with a simple passive variable pitch system predict a peak performance coefficient (efficiency) C_P of 0.47, a 50% increase over the same turbine with fixed pitch, along with an 8-fold increase in starting torque, shaking reduced by half and a large improvement in torque ripple. This prediction does not allow for radial arm drag losses, but [2] has measured a C_P of 0.5, as high as any reported for any form of HKT, with a combination of (i) active variable pitch and (ii) blades cantilevered from arms above water level, thereby eliminating arm drag losses. Several other measures have been shown to improve C_P, including improved blade profiles, reduced arm drag and blade tip losses, increased channel blockage, close-packed arrays of counter-rotating turbines, ducts and diffusers, and these are evaluated below.

High solidity and low tipspeed ratio result in low efficiency for fixed pitch Darrieus HKTs

Three factors lead to higher solidity σ in HKTs than in equivalent wind turbines: (i) Fluid dynamic forces are greater in water than in air, so HKT blades must generally be more robust, (ii) Wind turbine blade speeds are limited only by noise issues, but cavitation becomes an issue for HKT blades travelling at velocities relative to the water exceeding about 10 m/s (depending on blade profile, lift coefficient and depth of submergence). This limits λ to about 3 in a flow of 2.5 m/s. (iii) For Darrieus wind turbines, inertial ("centrifugal") forces typically exceed aerodynamic forces so the net force on blades acts outwards and slender troposkein blades which act in tension can be used without radial support arms, or at worst with slender low drag arms away from the equator. But in water, fluid dynamic forces generally exceed inertial forces and the net force on upstream blades is inward, so robust radial arms are unavoidable and parasitic drag losses from these arms increase steeply with λ, as shown by [3]. High σ in turn leads to peak C_P being reached at lower λ. It has been found in practice that optimum C_P is generally achieved at λ between 2 and 3 (see for example [4]). Fixed pitch blades stall at λ below about 3, greatly reducing efficiency and causing shock loading.

Improvements with variable pitch

Fixed pitch HKTs with both straight and helical blades were tested in open water by mounting in front of a vessel and driving the turbine through still water at a controlled speed. They were found to have very little starting torque and peak C_P no higher than 0.25 [5]. A 2-D double multiple streamtube (DMST) model (i.e. one without allowance for parasitic arm drag effects) was adapted to model the performance of fixed and variable pitch straight blade HKTs, and as mentioned above, indicated substantial improvements in starting torque, peak C_P, shaking and torque ripple [1]. Open water tests by the present author on a similar sized but not identical turbine with passive sinusoidal variable pitch showed C_P up to 0.31, a 24% improvement over fixed pitch, with much improved starting torque and reduced shaking. Measured C_P was lower than predicted, probably due to parasitic drag. Tests on a vertical axis wind turbine with a similar passive sinusoidal pitch mechanism also showed a marked improvement in starting torque.

Numerous sophisticated systems for active variable pitch, such as that used by [2] involving sensors, microprocessors and stepper motors to maintain optimum blade pitch and angle of attack α for all λ have been patented, but the present author believes that these are not necessary because tidal flow velocities change only slowly and the torque load on the turbine can be controlled so as to track the optimum λ, so that only one pitch regime is needed to give optimum α at optimum λ, and this can be achieved with a simple cam mechanism.

Reducing parasitic drag losses

Measurements by [4] show that parasitic loss due to blade tip losses and drag on the radial arms supporting the blades can be very serious, especially at higher λ, but can be minimised by (i) using arms with low drag and (ii) attaching arms to the ends of the blades rather than at points in from the ends which minimise blade bending moments. [2] has shown that C_P up to 0.5 can be achieved by a combination of active variable pitch and blades cantilevered from arms above water level, thereby eliminating arm drag losses. But this greatly increases blade bending moments and is probably feasible only in calm water.

Close packing, counter-rotating turbines, channel blockage, ducts and diffusers

[6] reports a 25% increase in the power output of 2 turbines if they are counter-rotating and placed close together. An array of close-packed counter-rotating turbines across the flow would be feasible at sites where the flow direction reverses. Such an array could achieve significant blockage and high C_P as reported by [7] in a narrow channel with high impedance, as discussed by [8], where this blockage would not significantly reduce flow and upset ecosystems.

[9] reports power augmentation factors up to about 4 on an axial flow wind turbine model with a duct and flanged diffuser, and it is likely that similar results could be achieved with a single cross flow HKT, but this power augmentation is achieved by drawing in flow from an area larger than the turbine swept area, which would not work with close-packed turbines. Also the diffuser structure is large and unidirectional, and would require fairly wide turbine spacing to enable it to yaw to follow reversing flows. A simple symmetrical duct tested by [4] increased turbine output by up to 74% and torque ripple was reduced at $\lambda \geq 2.75$, but increased at lower λ. However [10] found at $\lambda = 2$, use of a slightly different shaped duct reduced the torque ripple by a factor of 4.15 and the Cp increased by 57%. It appears therefore that there is room for further investigation of the effect of duct profile on torque ripple.

Conclusions

Straight blade Darrieus HKTs with simple passive pitch control, close packed, possibly with fairings which double as symmetrical ducts around support structures, offer a combination of low cost of construction with enhanced power output. In high impedance channels, high blockage can greatly increase power output.

References:

[1] Lazauskas, L. and Kirke, B.K. (2012). Modeling passive variable pitch cross flow hydrokinetic turbines to maximize performance and smooth operation. *Renewable Energy, Vol 45, 41-50.*
[2] Water Power Industries Norway. http://www.wpi.no/. Accessed 22/2/2014.
https://circle.ubc.ca/bitstream/handle/2429/14706/ubc_2008_spring_rawlings_george.pdf. Accessed 22/2/2014.
[3] Marsh, P., Ranmuthugala, D., Penesis, I. and Thomas, G. (2012). *Three Dimensional Numerical Simulations of a Straight-Bladed Vertical Axis Tidal Turbine.* 18th Australasian Fluid Mechanics Conference Launceston, Australia, 3-7 December.
[4] Rawlings, G.W. (2008). *Parametric characterization of an experimental vertical axis hydro turbine*. BASc, University of British Columbia.
[5] Kirke B.K, (2011). Tests on ducted and bare helical and straight blade Darrieus hydrokinetic turbines, *Renewable Energy* 36, 3013-3022.
[6] Ye Li and Calisal, S.M. (2010). Modeling of twin-turbine systems with vertical axis tidal current turbines: Part I - Power output. *Ocean Engineering* 37, 627–637.
[7] McAdam, R.A., Houlsby, G.T. and Oldfield, M.L.G. (2013). Experimental measurements of the hydrodynamic performance and structural loading of the Transverse Horizontal Axis Water Turbine: Part 1. *Renewable Energy* 59, 105-114.
[8] Salter, S. (2013). Are Nearly all Tidal Stream Turbines Designs Wrong? *Second Oxford Tidal stream Workshop.*
[9] Ohya, Y., Karasudani, T., Sakurai, A., Abe, K. and Inoue, M. (2008). Development of a shrouded wind turbine with a flanged diffuser. *J. Wind Engineering and Industrial Aerodynamics* 96, 524–539.
[10] Malipeddi, A.R. and Chatterjee, D. (2012). Influence of duct geometry on the performance of Darrieus hydroturbine. *Renewable Energy* 43, 292-300.

Wave Induced Loads and Kinematics for Turbine Support Structures in Turbulent Flow

A. Olczak, E. Fernandez Rodriguez, T. Stallard and P.K. Stansby
School of Mechanical, Aerospace and Civil Engineering, University of Manchester, M13 9PL

Summary: A series of experiments has been conducted to assess the magnitude of turbine loads due to waves relative to those due to turbulence only and to determine the characteristics of the flow incident to downstream turbine locations. The distribution of thrust force on a single rotor in turbulent flow is fitted to an extreme value distribution and the modification due to opposing waves determined. The flow-field downstream of a single turbine and a fence of five discs is also studied to inform the loading on downstream turbines.

Introduction

Unsteady loads due to turbulence and due to waves are important design consideration for developers of tidal stream turbines and their supporting infrastructure. For isolated turbines the prediction of such loads is dependent on characterisation of the ambient flow and on the mode of operation of the turbine. In particular, above rated power pitch or stall control may be employed to limit mechanical loads. Blade and rotor loads have been analysed by blade element momentum theory, CFD, and laboratory experiments (e.g. [1-3]) typically with low values of onset turbulence. For turbines within arrays, the incident flow may be dependent on the wake of other turbines within the array and wave conditions may vary as they propagate across farms. Numerical and experimental studies of wakes have shown dependence of recovery on ambient turbulence characteristics [4] and numerical approach [5] but there have been limited studies of the influence of waves on the flow field downstream of turbines. The present study addresses the influence of waves on the loading and resultant wake of turbines that are subject to a flow with turbulence representative of a tidal stream site. Loading is studied for a single turbine and the downstream flow considered for both a single turbine and a small fence.

Experimental Arrangement

Time variation of wake velocity and of the corresponding thrust force were measured on model tidal turbines of diameter D = 0.27 m in water depth h = 0.45 m due to a turbulent flow and due to the same flow with opposing waves. The arrangement was similar to earlier studies by the authors [6] with turbine represented using a single three bladed rotor and up to five identical porous discs with porosity selected to develop the same thrust coefficient. The rotor or central disc was located at mid-span of an open channel of width 5 m and depth 0.45 m and 6 m downstream of a porous inflow weir and 6 m upstream (and upwave) of a line of flap type wave paddles. For all cases, the mean velocity of the flow is 0.46 m/s. At hub height (mid-depth), the flow had turbulence intensity of 12% and streamwise length scale was in the range 0.25-0.267 m. Waves generated had wavelength $L = 4.5h$ to $6h$ and amplitudes of $A = 0.035h$ to $0.08h$.

Rotor Loading

For a single turbine the mean thrust due to waves opposing turbulent flow was within 2% of the mean thrust due to flow only. An extreme value analysis was conducted to obtain the magnitude of thrust with 1 in N probability of exceedance. The peak force F_i during n = 1 to N independent events during a record of $0 < t < M$ is identified. The probability of exceedance of a given force is then $P(F > F_i) = n(F > F_i)/N$. Alternative extreme value distributions were compared and sensitivity to threshold force and sample interval analysed to obtain convergence to within 3%. The 0.1% load due to turbulent flow was found to be 50% greater than the mean thrust. The extreme values due to waves and turbulent flow were found to depart from the turbulent thrust distribution and exhibited a quadratic growth with velocity amplitude. It is found that a reasonable prediction of the extreme forces due to both turbulence and waves is given by superposition of a drag force with drag coefficient of 2 based on the wave particle velocity only and with an unchanged mean thrust coefficient of 0.89 for the turbulent flow.

Wakes and Waves

Measurement of velocities downstream of a single rotor showed the periodic wave-induced fluctuations altered the depth profile of both mean velocity and total kinetic energy of the flow (here denoted FKE) within 4D downstream (Fig. 1). As might be expected the depth over which the wake velocity profile was altered is dependent on the wave depth parameter kh. The superposition of waves was also found to increase the rate of

recovery of mean velocity along the axial centreline to a distance of 10D downstream. Measurements within the wake of multiple turbines show very similar wake profile and recovery rate without and with waves. In part this is due to a reduction of wave height over the reduced velocity region downstream of the turbines (Fig. 2). This is attributed to wave refraction across the transverse shear profile that exists between the wake and bypass flow. Preliminary analysis of this process using the spectral wave model SWAN will also be presented.

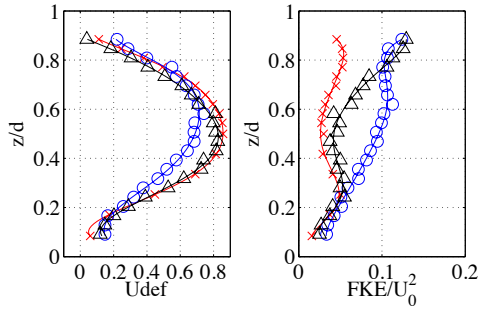

Figure 1: Depth profile of velocity deficit and of kinetic energy of the flow (turbulent and wave induced) measured 2 Diameters downstream of a 3-bladed rotor with thrust coefficient 0.89 and tip speed ratio 5.5. (x - No Wave, o – kd=1 and Δ - kd=3.13)

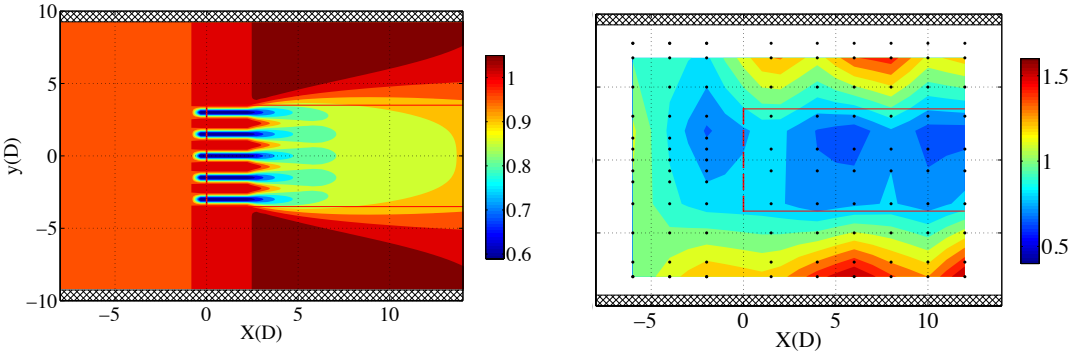

Figure 2: Velocity deficit field (left, 1-U_x/U_0) from empirical wake model and change of significant wave height (right, H_s/H_{s0}) in vicinity of a row of five discs. Disc are at centre to centre spacing of 1.5D with central disc at (x,y) = (0,0).

Conclusions

Load and flow measurements from scale experiments using a rotor, discs and a wide channel have been analysed to understand the extent to which turbine loading may be influenced by waves at tidal stream sites. The thrust exceeded with probability 1 in *N* was analysed for turbulent flow only and with waves. A reasonable prediction of the load distribution in waves is given by the turbulent load distribution superposed with a drag force based on the wave-induced kinematics only. Downstream of a single turbine waves are observed to increase the total kinetic energy to a depth dependent on the wave depth parameter. This modifies the depth profile of velocity through the turbine centreline, particularly near the surface, and slightly alters the rate at which velocity recovers to the far-wake deficit. For multiple turbines, waves are reduced over the wake region and so the wake characteristics are comparable both without and with waves.

References:

[1] Faudot, C and Dahlhaug, D (2012) "*Prediction of Wave Loads on Tidal Turbine Blades*". Energy Procedia, 20, 116 - 133

[2] McCombes, T et al (2013) "SUPERGEN Marin Research: Modelling Wave Induced Flow Effects on Tidal Turbines". Proc 10th European Wave and Tidal Energy Conference, Aalborg, Denmark. Paper No.

[3] Baltrop,N., et al. (2007) "*Investigation into wave-current interactions in marine current turbines*". Proc. IMechE, Part A: J. of Power and Energy, 221 (2), 233-242

[4] Maganga, F., et al. (2009) "*Experimental characterisation of flow effects on marine current turbine behaviour and on its wake properties*", IET *Renewable Power Generation*, *4*(6), 498–498

[5] McNaughton, et al. (2012) "*CFD Prediction of Turbulent Flow on a Laboratory Scale Tidal Stream Turbine using RANS modelling*", Proc. 1st AWTEC, Jeju Island, Korea.

[6] Stallard, T., et al. (2013) "*Interactions between tidal turbine wakes: experimental study of a group of three-bladed rotors*". Phil. Trans. R. Soc. A 2013 **371**, 20120159

An Evaluation of Blockage Corrections for a Helical Cross-Flow Turbine

Robert Cavagnaro*, Brian Polagye
Northwest National Marine Renewable Energy Center, University of Washington, USA

Summary: The ability to accurately evaluate hydrokinetic turbine concepts at small-scale in experimental facilities is important for the development of new devices. Problems introduced by working at lab-scale include operation in a transitional Reynolds number regime and cross-sectional blockage. These factors are shown to influence performance characteristics of a helical cross-flow turbine tested over a range of inflow velocities in two experimental flumes. Published blockage corrections are applied in an attempt to match performance under conditions of varying blockage (constant inflow velocity) and varying inflow velocity (constant blockage).

Introduction

Small-scale testing of hydrokinetic turbines informs design decisions (e.g., number of blades, solidity, hydrofoil profile) during device development. This requires that performance characteristics of a small-scale device be reflective of full-scale performance and independent of the test facility. The presence of confining fluid boundaries in experimental flumes (and in natural channels) is known to influence performance by increasing mass flux through the turbine swept area [1]. Operation of a turbine in a transitional Reynolds number regime has also been shown to introduce a velocity dependence that results in a family of characteristic performance curves [2]. Research on corrections for cross-sectional blockage of a model in a flow (primarily for wind tunnel testing) has been conducted since the 1930s, starting with Glauert [3]. Pope & Harper provide rules for blockage corrections for bluff bodies and also "unusual shapes" [4]. An iteratively solved blockage correction based on actuator disc theory derived during a study on tidal turbine performance in a closed tunnel section is presented by Bahaj et al. [5]. Werle [6] describes a relation between peak performance and blockage (a conclusion also reached in [1]) and assumes that all points on a characteristic performance curve behave similarly to arrive at a correction based solely on the ratio of turbine swept area to channel cross-sectional area. Other blockage corrections have been proposed, but require parameters not generally quantified during experimental testing (i.e., wake diameter).

The focus of this study is to compare the performance curves of a small-scale helical cross-flow turbine tested in two experimental flumes at different velocities and blockage ratios. The blockage corrections of Pope & Harper, Bahaj et al., and Werle are applied to the experimental results and compared.

Methods

The small-scale turbine experiments referenced herein are previously described [2]. Experimental apparatus and the geometry of the flumes at the University of Washington (UW) and Bamfield Marine Science Centre (BMSC) lead to experiments with blockage ratios, defined as

$$\varepsilon = \frac{(A_{Turbine} + A_{Rig})}{A_{Channel}}, \tag{1}$$

that range between 9% and 19%, where A_{Rig} is the cross-sectional area of the test rig supporting the turbine. Turbulence intensity for experiments at the UW flume is 3% compared to 10% at BMSC. Velocities range from 0.55 – 0.70 m/s (UW) and 0.55 – 1.0 m/s (BMSC) with average water depths of 0.5 m (UW) and 0.8 m (BMSC). Chord length Reynolds numbers are transitional in both cases (10^4-10^5).

All blockage corrections relate the equivalent unconfined "free" velocity (U_F), coefficient of performance ($C_{P,F}$, and tip-speed ratio (λ_F) to blocked "tunnel" values measured in an experiment [5] (U_T, $C_{P,T}$, λ_T) as

$$U_F = U_T \sqrt[3]{\frac{C_{P_T}}{C_{P_F}}}, \; C_{P_F} = C_{P_T}\left(\frac{U_T}{U_F}\right)^3, \; \lambda_F = \lambda_T\left(\frac{U_T}{U_F}\right) \tag{2-4}$$

where,

$$C_P = \frac{P}{0.5\rho A_{Turbine} U^3}, \; \lambda = \frac{R\omega}{U} \tag{5-6}$$

in which P is the mechanical power produced by the turbine, ρ the water density, R the turbine radius, and ω the turbine rotation rate. The relation between U_T and U_F depends on the correction employed and is a function of ε [4,6] or ε and the thrust coefficient ($C_T = T/0.5\rho A_{Turbine} U^2$) [5]. A critical assumption for the latter is the tunnel disc flow speed, rpm and thrust are the same as in the unconfined case [5].

* Corresponding author.
Email address: rcav@uw.edu

Results

Blockage corrections by Werle, Pope & Harper, and Bahaj et al. are applied to experimental measurements shown in Figure 1. Without correction, performance depends on inflow velocity and blockage, with increases in either parameter shifting peak performance towards higher C_P and greater λ. All corrections somewhat reduce the absolute scatter between curves for the constant blockage case. The Werle correction appears to significantly reduce scatter for the constant velocity case (Fig. 1*e*), while the other two reduce scatter, but to a lesser degree.

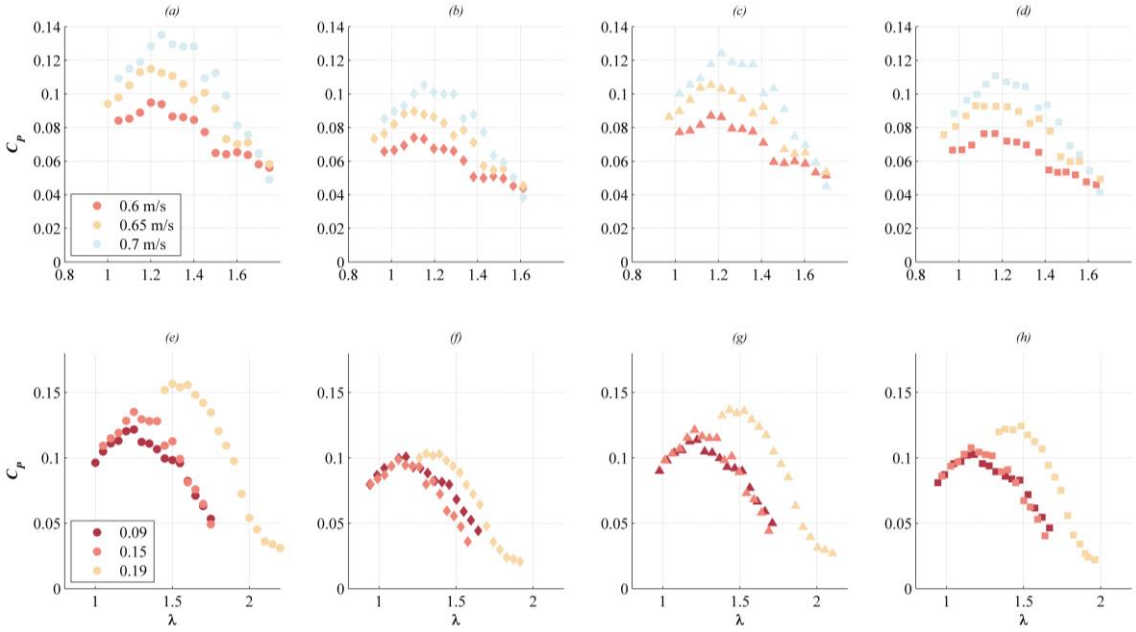

Fig. 1: Performance at same blockage (ε = 15%) varying speed (top). Uncorrected (*a*) and with Werle, Pope & Harper, and Bahaj et al. corrections *(b)-(d)*, respectively. Performance at same speed (0.7 m/s) varying blockage (bottom). Uncorrected (*e*) and with Werle, Pope & Harper, and Bahaj et al. corrections *(f)-(h)*, respectively.

Conclusions

Corrections are shown to reduce variation in performance curves at different levels of blockage. None of them are universally effective, likely because none of these corrections account for the full physics present in the confined flow problem. For this reason, care should be taken when choosing or applying a blockage correction. At transitional Reynolds number, the effect of blockage is likely to be convolved with the Reynolds number dependence of unsteady lift and drag. Both of these effects highlight the challenge of estimating full-scale, unconfined performance from small-scale testing.

Acknowledgements:

The authors would like to acknowledge support from Dr. Roy Martin, funding from the US DOE under DE-FG36-08GO18179, Fiona Spencer of UW, and Dr. Eric Clelland of BMSC.

References:

[1] Garrett, C., & Cummins, P. (2007). The efficiency of a turbine in a tidal channel. *Journal of Fluid Mechanics*, *588*, 243–251. doi:10.1017/S0022112007007781

[2] Polagye, B., R. Cavagnaro, and A. Niblick (2013) Micropower from Tidal Turbines, *ASME Fluids Division Summer Meeting*, July 8-11, 2013, Incline Village, NV.

[3] Glauert H. (1947). *The Elements of Aerofoil and Airscrew Theory*, 2nd ed. New York: Cambridge University Press

[4] Pope A, Harper JJ. (1966) *Low-Speed Wind Tunnel Testing*, 2nd ed. New York: Wiley

[5] Bahaj, a. S., Molland, a. F., Chaplin, J. R., & Batten, W. M. J. (2007). *Power and thrust measurements of marine current turbines under various hydrodynamic flow conditions in a cavitation tunnel and a towing tank*. Renewable Energy, 32(3), 407–426. doi:10.1016/j.renene.2006.01.012

[6] Werle, M. J. (2010). *Wind Turbine Wall-Blockage Performance Corrections*. Journal of Propulsion and Power, 26(6), 1317–1321. doi:10.2514/1.44602

Numerical Modelling of a Gorlov Cross Flow Tidal Turbine

Esther R. Bruce
Department of Engineering Science, University of Hull, UK

Summary: The aim of this study is to simulate the experimental data as a Computational Fluid Dynamic (CFD) numerical model in order to accurately validate against experimental work. The experiment selected was conducted by A.L.Niblick at the University of Washington's NNMREC [1]. Obtaining a greater understanding of the impact a Gorlov cross flow tidal turbine has on the flow structure around the turbine and the wake downstream is vital to optimise the design and improve power generation. The CFD commercial code used in this three dimensional simulation is StarCCM+ 9.02.005, with a k-ω Shear Stress Transport (SST) turbulence model.

Introduction

The demand for non-fossil fuel power alternatives that are efficient and commercially viable is leading to increasing research into extraction of kinetic energy produced by current and flow streams. A Gorlov is the type of cross flow turbine investigated within this project, the cross flow turbine axis is perpendicular to the free stream velocity. This was first developed in 1995 by A.M.Gorlov and is a unidirectional helical turbine in which the blades span an azimuthal range of 90 degrees [2] as represented in figure 1.

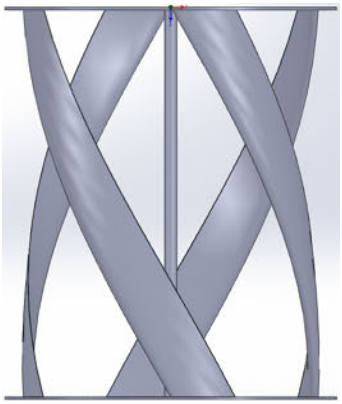

Figure 1 Gorlov Turbine

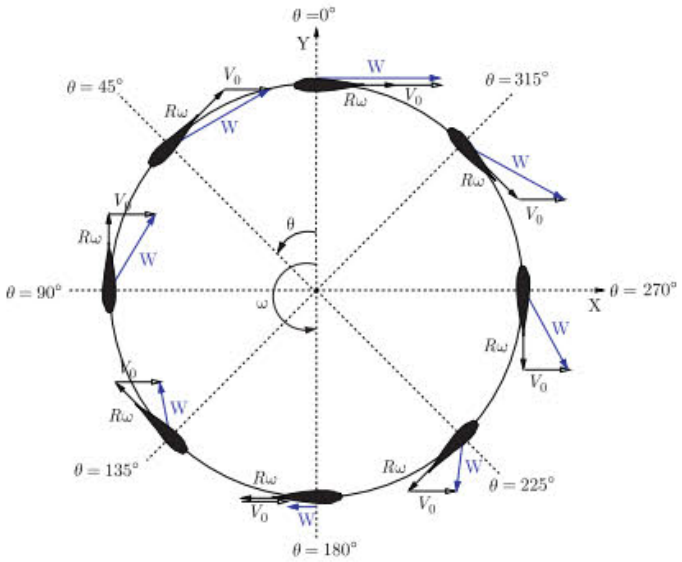

Figure 2 Turbine Positioning [3]

The main advantage of the Gorlov turbine is that it produces a uniform torque distribution. Unlike a Darrieus turbine, which has straight blades and produces a non uniform circumferential torque distribution. The Gorlov's uniform torque distribution is due to the simultaneous position of each of the turbine blades being in every azimuthal position. The shaft torque is kept constant due to the helical configuration that ensures that the portions of the blade generate positive torque which rotates the turbine at a continuous speed.

Figure 2 illustrates a cross sectional view of a hydrofoil in eight different azimuthal positions. Resolving the free stream velocity (V_o) and the tangential velocity ($V_\theta = \omega R$, ω is angular velocity, R is the radius) means the resultant velocity is presented in equation below;

$$V_R = \sqrt{(V_o + V_\theta \cos\theta)^2 + (V_\theta \sin\theta)^2} \quad (1)$$

Methods

Primarily, the CFD methodology must first be fully validated against experimental data. The CFD geometry and flow conditions were generated so that the flume, turbine geometry and the fluid properties correspond to the experimental procedure of A.L.Niblick [1]. The lab-scale device has four NACA 0018 helical blades with two circular end plates, the diameter is 0.172m, 0.234m high, chord length of 0.04m and the solidarity (σ=Nc/zR) of

0.03. The mesh domain blockage ratio is 12% and is constant with the blockage ratio of the experimental data. The helical blades of the Gorlov turbine increase the complexity of the mesh and in order to resolve the near wall flow accurately prism layers are generated around the hydrofoil.

Initially a single three dimensional static blade at varying azimuthal positions was simulated. Detailed mesh refinements and an investigation of y+ values were performed on the single blade to allow for computational cost to be kept to a minimum. A three dimensional rotating turbine is currently being simulated at a tip speed ratio of 1.6 with a fixed angle of velocity and an inlet velocity magnitude of 0.7m/s. The CFD simulation is based on Reynolds-Average Navier-Stokes with a K-omega SST turbulence model, second order accuracy time and space discretisation. An investigation into the grid sensitivity was conducted with a fine mesh (12 million cells) and a coarse mesh (6 million cells).

Results

Initial simulations have produced encouraging results in which there are similar trends to that of the experimental data. It is necessary to generate a fine mesh capturing both the far field and the near wall boundary layer, as this is essential to the accurate prediction of the forces and the separation phenomena. Thus it is vital to produce an acceptable wall distance from the airfoil and the first prism layer. A variation in y+ values on a helical blade can be seen in figure 3. Ideally the magnitude of the first prism layer thickness is constructed in order to create y+ values of less than 1.

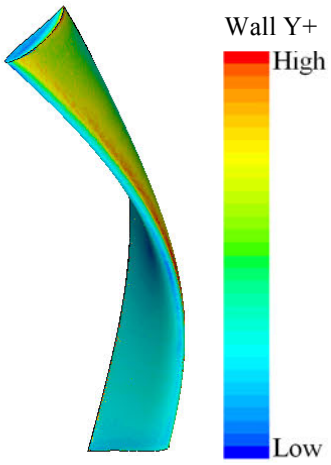

Figure 3 Y+ Values on the blade

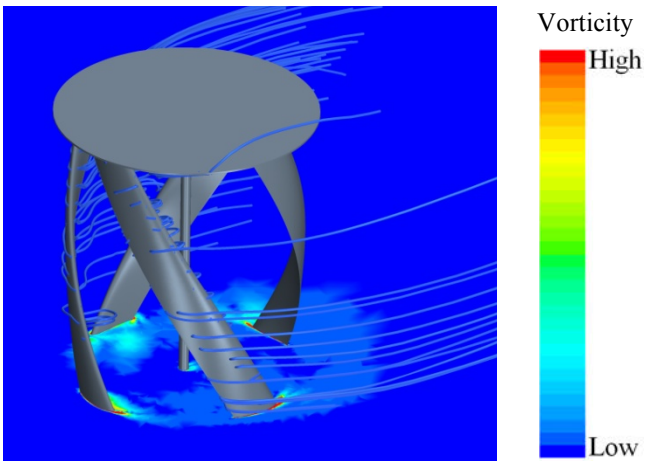

Figure 4 Streamlines and Vorticity around the blades

Low y+ values are vital, however, reducing the first prism layer thickness can result in the increase of the number of cells within the mesh thus increasing the computational cost. The cut-plane in figure 4 shows the vortices which occur around the turbine blades and the streamlines show a snapshot of the wake generated by the blades.

Conclusion

An ongoing mesh refinement is currently being conducted in order to increase the accuracy of the computer simulation, before optimization work can begin on the turbine. Tidal turbines will be a fundamentally important component of energy production in the near future. Further extensive research has to be undertaken in the area of cross flow turbines thus enabling them to realise their potential in the renewable energy sector.

References:

[1] A.L.Niblick, Experimental and Analytical Study of Helical Cross-Flow Turbines for a Tidal Micropower Generation System. Master's thesis, University of Washington. 2012

[2] A.M.Gorlov, inventor Unidirectional helical reaction turbine opterable under reversible fluid flow for power systems. USA1995.

[3] T.J.Hall, Numerical Simulation of a Cross Flow Marine Hydrokinetic Turbine. Master's thesis, University of Washington. 2012

Numerical modelling of sea bed morphodynamics associated with tidal energy extraction

Antonia Chatzirodou, Harshinie Karunarathna
Engineering from Clouds to Coast Research Group, College of Engineering, Swansea University, Swansea, SA2 8PG

Summary: Tidal energy generation is an option favoured by the UK Government towards its initiative to generate renewable energy. Since the industry is now moving toward - tidal array devices deployments, it is important to investigate environmental impacts associated with tidal energy extraction. As a result, it is essential that a good understanding is gained upon altered residual flows connected to sediment transport regime and perturbed vertical velocity profiles controlling sediments in suspension, and effects of tidal array installations on sea bed sedimentary features, before reaching commercialization [1]. In the present study Delft3D coastal area morphodynamic modelling suite is used to investigate hydrodynamic and in subsequent morphodynamic aspects of tidal energy extraction. Initial results indicate that morphodynamics in areas considered for tidal turbines deployment are in a dynamic equilibrium. In such a dynamic environment, results imply that possible alterations in tidal currents due to energy extraction may have some implications on existing morphodynamic regime.

Introduction

UK is ideally located to exploit marine renewable energy resources. Tidal energy generation is an option favoured by the UK Government [2]. It is thus vital that local and regional environmental impacts of tidal energy extraction are well understood. However, potential impacts that arrays of tidal current turbines may have on the surrounding coastal environment is still largely unknown. Particular concerns are the extent to which the altered tidal environment as a result of energy extraction will change the natural sediment transport regime and hence the sea bottom morphodynamics, which may have some implications on the stability of nearby beaches and sea bed ecology [3].

In the work presented here, Delft3D coastal area morphodynamic modelling suite is used to investigate hydrodynamic and morphodynamic aspects of tidal energy extraction. Pentland Firth (PF) channel between Scottish Mainland (UK) and Orkney Islands, joining Atlantic Ocean with the Northern Sea, is used as a test site. Due to different tidal ranges and phase at the ends of the channel, tidal currents of up to 8 m/s are generated in places in response to 2.5 m head drop [4], providing a substantial energy resource for turbine deployments [5,6]. Concerning sea bed morphology, a sandbank , located eastwards in Inner Sound Channel is of particular interest (Fig.1).Hydrodynamic boundary conditions established from a large scale flow model produced appropriate boundaries for nested areas favoured for tidal energy extraction (blue area marked in Fig. 1). Hydrodynamics of the model were validated against measured flows at 3 locations within the model domain (Fig. 2). Sensitivity tests were carried out on tuneable model parameters allowing confidence into investigating impacts of tidal energy converters on sea bed morphology.

Numerical Modelling and Results

In terms of flow modelling a full calibration analysis has been conducted so that an appropriate combination of Delft3D flow parameters could be applied in the area of interest. Hydrodynamic conditions of a large scale model (Fig. 1-domain (a)), covering the whole area of PF, were modelled and compared against ADCP measurements at 3 sites (Fig. 2, 3). Hydrodynamics of the large scale model provided appropriate boundary conditions for the nested, high resolution model (Figure 1 –domain (b)), which covers the areas favoured for tidal energy exploitation.

A good agreement is found between the modelled and measured values of current velocities at 3 ADCP sites. Observed deviations from ADCP records may be attributed to wave–current interactions. Baroclinic effects and stratification effects which may disturb the logarithmic vertical velocity profile were not taken into account in the present study. It should be noted that overall model output seems to be significantly sensitive to bed friction where a constant Chezy value of 50 $m^{(1/2)}$/sec is eventually selected.

Even though the sea bed in PF is mainly rocky, vast sand deposits are abundant in some areas. The sandbank (Fig. 1) is a large sand/gravel deposit located in this area. Into that sandy area highly mobile gravel form large sandy ripples, superimposed on small sand waves. To investigate the naturally occurring sediment dynamics in this area, a nested morphodynamic model, covering the Inner Sound Channel, was set up. The complex patterns of sediment distribution were encapsulated by considering varying sediment grain size and mobile seabed thickness. Sand coverage within the selected computational grid was produced via data

interrogation accessed by Marine Scotland video trawls, BGS particle size processed data and mapped Geological conditions available by Meygen EIA Quality Mark Report [7]. Preliminary investigation of existing morphodynamics of the sandbank area during a full spring-neap tidal cycle shows that it is extremely dynamic. During the flow and ebb phases of the tidal cycle, transient eddies are apparent between the tip of the island of Stroma (Fig.1) and over the sandbank, indicating a possible connection between those transient tidal patterns and the formation and maintenance mechanisms of the offshore sandbank. At spring flood phase where velocities reach their maximum (up to 2.8 m/s), strong currents occur generally offshore of the southern flank of the sandbank. Currents flow towards the E-NE, being clearly affected by the presence of the Island of Stroma. At the same time, mean total sediment transport rates demonstrate increasing gradients towards the southern flank of the sandbank area.

Conclusions

Preliminary investigations indicate that sea bed morphology of sandy areas in PF is sensitive to hydrodynamics. Locations favoured for tidal energy extraction lie in proximity to highly sensitive sand/gravel deposits. As a result, it is important to investigate the impacts of tidal energy extraction on the hydrodynamics and the morphodynamics of this area. Numerical modelling study is still underway to investigate the linkage between the complex current patterns and the existing sediment transport regime. Following that, the models will be used to investigate the impacts of tidal current turbines on sea bed sediment dynamics.

Acknowledgements:
The authors wish to acknowledge College of Engineering of Swansea University and Low Carbon Research Institute for the financial support provided for this research. EPSRC funded Terawatt project EP/J010170/1 is greatly appreciated for providing data.

References:

[1] Robins, P.E. (2013). Influence of tidal - stream energy extraction on sediment dynamics. In EWTEC Conference 2013, Denmark.
[2] Bryden, I.G. (2006). The marine energy resource, constraints and opportunities. Proceedings of the ICE - Maritime Engineering, Volume 159, Issue 2, 55 –65.
[3] Neill, S.P., Jordan, J.R. & Couch, S.J. (2012). Impacts of tidal energy converter arrays (TEC) on the dynamics of headland sand banks. Renewable Energy, 37, 387-397.
[4] Bowyer, P. & Marchi, G. (2011). Tidal Residual flows in the Pentland Firth. 9th European Wave and Tidal Energy Conference, Southampton, UK.
[5]Adcock T.A.A, Draper S., Houlsby G.T., Borthwick A.G.L and Serhadlıoğlu, S. 2013. The available power from tidal stream turbines in the Pentland Firth. Proc R Soc A 469: 20130072.
[6] Baston, S. & Harris, R.E. (2011). Modelling the Hydrodynamic characteristics of Tidal Flow in the Pentland Firth. In EWTEC 2011, Southampton, UK.
[7] MeyGen: Tidal Energy Project Phase 1 Environmental Statement. EIA Quality Mark Report

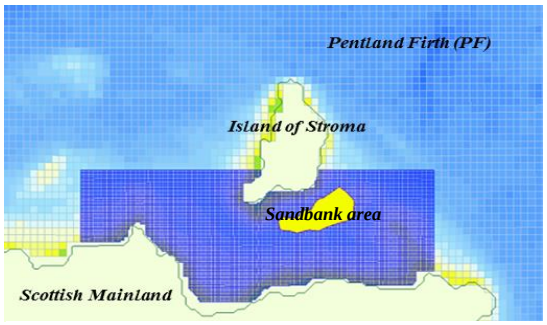

Figure 1: Sea bottom bathymetry inside PF

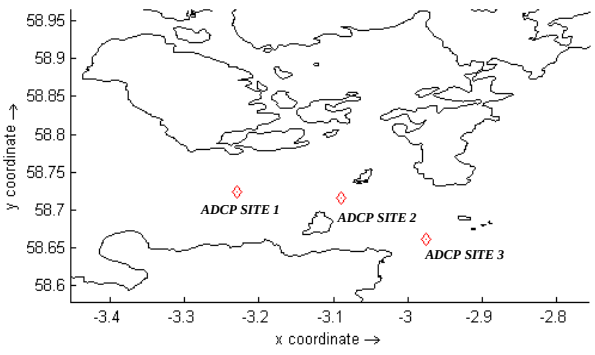

Figure 2: Location of ADCP record sites inside PF

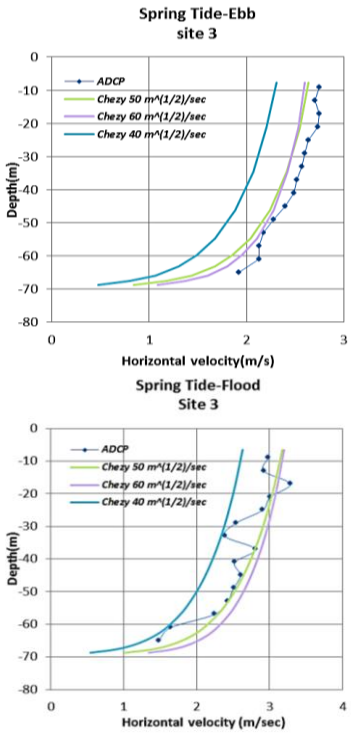

Figure 3: Calibration of flow model inside PF (Site 3)

Feedbacks between energy extraction and bed elevation morphodynamic

Andres Payo*, Jim Hall
School of Geography and the Environment, University of Oxford, UK

Summary: Anticipating the effect of tidal energy extraction on tidal basin morphodynamic over decadal time scales is required for coastal management purposes and commercial development planning over the useful life of the plant. Causal loop analysis is used here to explore the influence of tidal energy extraction on bed elevation morphodynamic. This qualitative analysis, suggested that erosion-deposition balances of weakly coupled bed sediments (i.e. coarse bed material or low energy environments) are the most affected by reducing the resilience (i.e. ability to return to original state of water depth) or even de-coupling it from hydrodynamic forcing.

Introduction

Natural variability and estimations of morphology changes with and without tidal energy extraction has been used to assess the importance of tidal energy extraction on bottom morphodynamic and sediment transport [1,2]. [1] conclude that energy extraction (of the order 10-20 MW) will reduce velocities and suspended sediment concentrations locally but considered these changes negligible for being an order of magnitude less than seasonal predicted variability. [2] Using model simulations suggested that the influence of tidal energy extraction on bed level change is more pronounced on regions of strong tidal asymmetry by affecting the erosion/deposition pattern over a considerable distance from the point of energy extraction. Extrapolating these results to decadal morphodynamic behaviour at basin scale is not trivial due to non-linarites and the lack of an up-scaling closure theory. Recently it has been shown how causal loop analysis can be used to assess the coastal system behaviour at decadal and longer time scales [3]. This method of analysis is used here to explore the impact of tidal energy extraction on the erosion-deposition balance.

Methods

First Causal Loop Diagrams are used to represent a distillation, from existing literature, of the feedback structure (at active layer scale) of a non-specific tidal basin system (Figure 1). Then, the influence of tidal energy extraction is included into the feedback structure and qualitative stability diagrams used to assess the system behaviour. To be consistent with the [1, 2], tidal energy extraction is conceptualized here as an extra energy dissipation process that varies non-linearly with the flow velocity. The energy extraction is represented as a positive link between the local depth-averaged wave-tides induced current velocity and the tidal energy extraction rate (Figure 1a). A positive influence indicates that an increase of current velocity increases the tidal energy extraction rate. To avoid cluttering the feedback structure this positive link is collapsed (i.e. product of positive and negative links) as a negative link between the local water depth (h) and the energy extraction rate. In contrast to wave and current energy dissipation rate due to bottom friction, tidal energy extraction rate has a negative influence on the erosion rate by reducing the near bed erosion potential. This is derived from the depth-averaged energy conservation and suspension model of [4]. Tidal energy extraction adds a new energy dissipation process to the energy balance indirectly reducing the sediment suspension efficiency. This difference introduces a new reinforcing feedback loop into the system that competes with the natural balanced erosion-deposition feedback loop (Figure 1b, blue and green loops respectively).

Results

Figure 2 illustrates three potential types of influences on the local erosion-deposition balances; (a) if the bed layer is not coupled with the hydrodynamic it will remains non-coupled if tidal energy is extracted; (b) if original stable and non-stable water depth are not well apart, tidal energy extraction might either reduce this distance further or even decoupling the bed from the hydrodynamics; (c) if the bed layer is coupled and the water depth at which unstable and non-stable erosion/deposition balances lies are well apart, the new depths will be only slightly modified.

* Corresponding author.
Email address: andres.payo@ouce.ox.ac.uk

Conclusions

Impacts of tidal energy extraction on bed layer dynamic are explored by reasoning on the feedback loop structure of morphodynamic processes at the active layer scale. It is shown how non direct effect are triggered influencing the overall feedback factor balance by adding a new reinforcing loop. Erosion-deposition balances of weakly coupled bed sediments (i.e. coarse bed material or low energy environments) are the most affected by reducing the resilience (i.e. ability to return to original state of water depth) or even de-coupling it from hydrodynamic forcing.

Acknowledgements:

This research was funded by UK National Environmental Research Council (http://www.nerc.ac.uk) with support from the Environment Agency (http://environment-agency.gov.uk) as part of the project: iCOASST. Integrating Coastal Sediment Systems.

References:

[1] Robins, P. E. (2013). Influence of tidal energy extraction on fine sediment dynamics. *Proc. 2nd Oxford Tidal Energy Workshop*, Oxford, UK, pp 27-28.

[2] Neill, S. P. (2013). Impact of tidal energy arrays located in regions of tidal asymmetry. *Proc. 2nd Oxford Tidal Energy Workshop*, Oxford, UK, pp 19-20.

[3] Payo, A., Hall, J., French, J., Sutherland, J., Maanen, B., Nicholls, R. J., Reeve, D. (in press). Causal loop analysis of geomorphological coastal systems. Special issue *Journal of Geomorphology*.

[4] Kobayashi, N., A. Payo, and L. Schmied, Cross-shore suspended sand and bed load transport on beaches. *Journal of Geophysical Research*: Oceans, 2008. 113(C7): p. C07001.

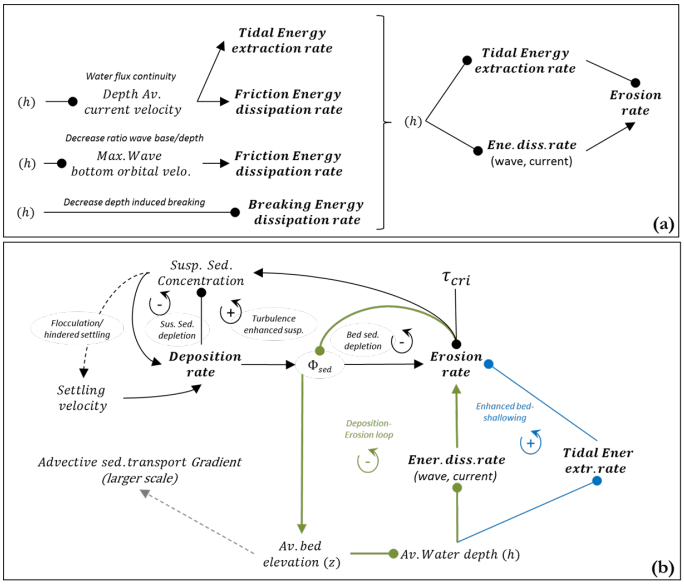

Figure 1. Tidal energy extraction within the feedback structure of tidal basin morphodynamic processes at the active layer scale. State variables are represented by text and positive/negative links between them as arrow or dot headed lines. The position of the line head represents the polarity of the link. Tidal energy extraction is represented as a positive link between the depth-averaged velocity and energy extraction (a). The influence of tidal energy extraction is collapsed into a negative link between average water depth and Energy dissipation rate. The overall feedback structure is represented in (b). Influence on local bed elevation on advective sediment transport is acknowledge but not represented (larger scale).

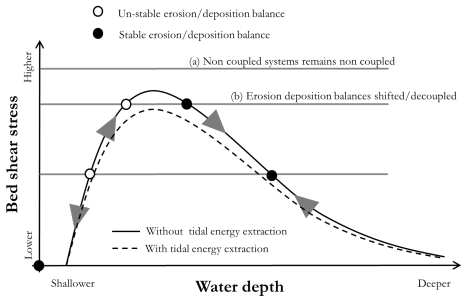

Figure 2. Anticipated influences of tidal extraction on the local erosion/deposition balance. The mean variation of bed shear stress due to wind and waves with the water depth is represented as a black curve. A dashed black curve represents the bed shear stress if tidal energy extraction is included. Noticed that due to non-linearity higher bed-shear stress are significantly more reduced than lower values. The critical shear stress needed to initiate sediment transport is presented by three horizontal grey lines. If critical shear stress crosses the bed shear stress curve, bed changes are coupled with hydrodynamic. When coupled, two stable and one unstable erosion/deposition balance might occur. The arrows indicate the direction of change.

Performing oceanographic surveys on tidal energy sites using a data buoy

Mungo Morgan
North Sea Systems Ltd, Dorset, Uk

Summary: A met-ocean survey buoy (*DataFish*®), invented by D Rigg (MEng Oxon.) has been developed by North Sea Systems to collect oceanographic data from tidal energy sites. This report discusses the development process of *DataFish*® beginning with the hydrodynamic modelling of the hull using *OrcaFlex*® (computer software for dynamic analysis of offshore marine systems). The electrical system including battery capacity, compatible sensors, data logging capabilities and data transmission methods are then discussed. *DataFish*® specifically targets current profiling through the use of Acoustic Doppler Current Profilers (ADCPs) and Acoustic Doppler Velocimeters ADVs), acoustic measurements with hydrophones and wave measurements with accelerometers.

Introduction

Collecting data from tidal energy sites is notoriously difficult primarily due to the speed of the tidal stream and the short working windows available during slack tide periods. There are many examples of failed surveys, where buoys are dragged under or break their moorings, or data is found to be of poor quality once the sensors are retrieved. *DataFish*® was designed to overcome these challenges by being hydrodynamically shaped, remaining stable in fast streams and providing real time access to the data it collects. *DataFish*® carries a 660Ah 12V battery bank, data logging and transmission capabilities making it a state of the art marine survey platform. This report discusses the engineering design process of *DataFish*® and future development work.

Design Methodology

The basis of design for *DataFish*® hull focussed on the survivability during tidal streams of up to 6m/s and significant wave heights of 5m. Other considerations that affected the hull design were the logistical requirements to transport and deploy the buoy and the need to accommodate electrical equipment within the hull. A naval architect was contracted to design the shape of the hull, which is fabricated from vacuum infused glass fibre. The environmental conditions and mooring line properties were used to define the initial *OrcaFlex*® model. Using the results of the hydrodynamic analysis an iterative approach was used to generate the minimum hull volume required for the buoy to remain on the surface worst case conditions, except for occasional submergence due to wave action. This model was then subjected to a variety of environmental load cases to generate peak loads and assess motions and stability during service and towing.

Electrical System

The importance of knowing that *DataFish*® is secure and operating successfully was paramount in the design of the system. Therefore, the data from the sensors is collated using a data logger, which then transmits the data to a web based data hosting service (cloud) using a General Packet Radio Service (GPRS) modem in order that the data can be retrieved remotely in real time. To date, the following sensors have been deployed:

- Global Positioning System (GPS) antenna for location monitoring
- Load Shackle to monitor the load in the mooring
- Anemometer for wind velocity measurement
- Accelerometer for determining wave height and frequency
- ADCP for current profiling
- Hydrophone for underwater acoustic surveys

The power consumption of this standard set-up is approximately 4 Watts depending upon the settings, which results in a maximum deployment duration of 66 days as shown in the equation below:

$$\begin{aligned} Battery\ Life\ (days) &= \frac{Battery\ Capacity\ (Ah) * Depth\ of\ Discharge(\%) * Voltage(V)}{Power\ Consumption\ (W) * Hours\ per\ day} \\ &= \frac{660 * 0.8 * 12}{4 * 24} \\ &= 66\ days \end{aligned} \quad (1)$$

Torpedo - Additional sensor housing module

In December 2013, *DataFish*® was deployed with *Torpedo*, a low drag structure connected via a linkage to the mooring line that housed a hydrophone, although it has a second purpose as an ADV housing. This configuration is shown in figure 1 below. The ADV or hydrophone can be positioned at a known height in the water column and although this height will vary proportionately with the water velocity it remains relatively stable and points into the direction of the flow. It is easy to envisage a number of ADVs being placed at various heights along the mooring umbilical. The hydrophone deployment proved that a baseline acoustic survey could be carried out using the torpedo as a housing and *DataFish*® as a source of power and data collection platform.

Further Development

North Sea Systems has recently been awarded a Technology Strategy Board (TSB) grant to develop *DataFish*® so that it can power and communicate with sensors on the sea floor. This will be achieved through the use of a special umbilical that will act as the mooring line as well as the transmitter of power and data. The buoy will also be fitted with a hydro generator and solar panels such that the system can be deployed for durations of up to 6 months without any human intervention. This project is due for completion at the end of August this year. Testing of the complete new system will be taking place in July this year. Stage gate tests are being conducted of individual components and modules to prove their performance in isolation.

Results

DataFish® has been tested in the Anglesey Skerries, North Wales and off the South coast of England near Poole and in The Solent. The harshest conditions were seen in The Skerries, with significant wave heights (H_s) of 2m and tidal streams in excess of 2.5m/s as shown in graph 1 below. The conditions in the South of England were H_s=1m and tidal streams of up to 2m/s. This was where the hydrophone trial deployment was carried out in collaboration with Kongsberg Maritime who processed the acoustic data and correlated shipping noise with shipping movements shown on Automatic Identification System (AIS) software.

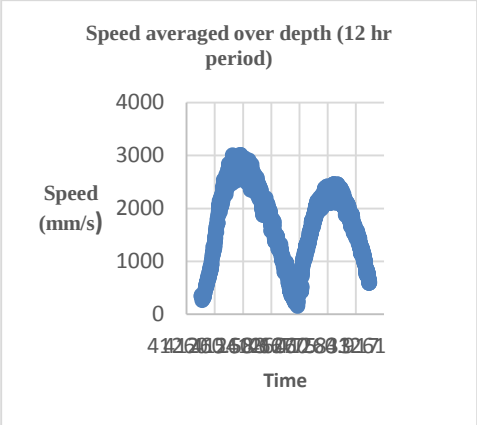

Graph 1 - Speed vs Time (Skerries)

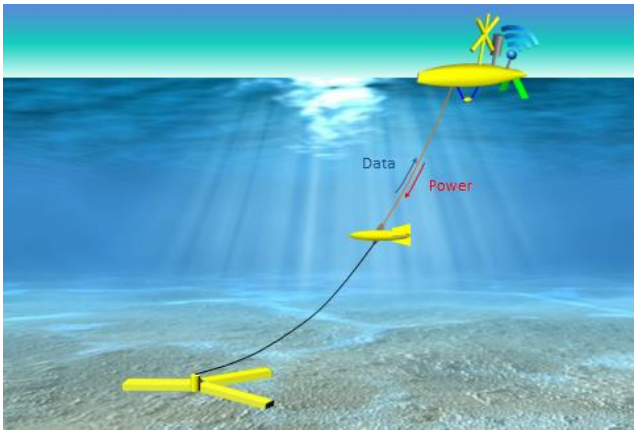

Figure 1 - DataFish, Torpedo and clump weight

Conclusions

A thorough design process was undertaken to develop the initial design of *DataFish*®. This design has not been validated at extremes but there is good correlation of the measured load shackle readings compared to those predicted by the *OrcaFlex*® model. *DataFish*® was monitored throughout the various trials and it was observed that the stability of the buoy improves as the water velocity increases. This is because a higher water velocity results in a higher mooring tension, and the mooring acts as a keel, with the mooring tension replacing the lead ballast. Data gathered to date has been of high quality and value to turbine developers and environmentalists. The TSB development project is on track for completion at the end of August this year and this will allow sensors to be bottom mounted and communicated with in real time.

Acknowledgements

Special thanks go to Alex Hewitt, the Naval Architect that designed the hull of *DataFish*®.

Quasi unsteady blade element momentum theory for tidal stream turbines

Thomas Nevalainen*, Cameron Johnstone, Andrew Grant
Energy Systems Research Unit, Dept. Mechanical & Aerospace, University of Strathclyde, UK

Summary: As tidal stream turbines (TSTs) enter the stage of full scale prototype testing, the understanding of the loads from surface waves and currents of these devices is critical to ensure high durability and confidence in designs [1]. Presented is a preliminary method of determining the hydrodynamic loads on TST blades operating in waves and shear current profile using blade element momentum theory (BEMT). The goal of the project is to use time-series load data obtained from BEMT and conduct a fatigue analysis using FEM software. Shown in this report is a case study of a TST operating in a rough sea state.

Introduction

Due to the inherent difficulties in conducting combined wave and shear current tests on TSTs, few methodologies are available for the prediction of dynamic loads caused by combined wave and current interactions [2]. A common practice in marine engineering is to linearly superimpose the water particle velocities caused by the waves and currents in order to calculate structural loads. This is however thought to be inappropriate due to the rotational flow of a non- linear current profile used in combination with wave models based on potential theory [3]. Studies conducted by Wang (1997) [4] indicate that the coupled wave and current interactions give as much as 30% higher maximum loads on submerged structures as the individual superimposed wave and current loads. This suggests that it would be appropriate to incorporate a more sophisticated wave- current model into the methods of load prediction in order to accurately represent the TST's real operating conditions. The methodology chosen by the author to determine the cyclic and peak loads on TSTs in the combined wave- current environment, is to use a BEMT scheme in combination with a 3rd order Stokes' wave theory coupled with a linear shear current. Since the BEMT method was originally developed for steady state operation, several modifications must be made to it in order to accommodate for the dynamic inflow caused by the surface waves and tidal velocity profiles. A summary of the method is given in the next section.

Modified BEMT scheme

The main principle of the BEMT method is to equate the thrust and torque forces exerted on the fluid to the ones exerted on the TST blades along a annular stream tube. The annular thrust, $\mathrm{d}F_\mathrm{a}$, and torque, $\mathrm{d}T_1$, on the fluid are expressed as

$$\mathrm{d}F_{\mathrm{a}1} = 2\pi r \frac{1}{2}\rho U^2 4a(1-a)\mathrm{d}r. \tag{1}$$

$$\mathrm{d}T_1 = 4b(1-a)\frac{1}{2}\rho U\Omega r^2 2\pi r\mathrm{d}r. \tag{2}$$

$$\mathrm{d}F_{\mathrm{a}2} = N\frac{1}{2}\rho V^2 c(C_\mathrm{L}\cos\phi + C_\mathrm{D}\sin\phi)\mathrm{d}r \tag{3}$$

$$\mathrm{d}T_2 = N\frac{1}{2}\rho V^2 cr(C_\mathrm{L}\sin\phi - C_\mathrm{D}\cos\phi)\mathrm{d}r \tag{4}$$

where a and b are the axial and tangential induction factors, Ω is the angular velocity of the rotor, r is the radial distance of the annular section, U is the free stream velocity, N is the number of blades, V is the resultant flow, c is the blade section chord length, ϕ is the angle of the resultant flow and $\mathrm{d}r$ is the annular section thickness. The equations are set equal and solved through iteration of a and b and the elemental forces are added up. Details of the derivation of these equations can be found in [5]. To account for the spatial velocity variations across the rotor plane, each annular stream tube is divided into azimuthal sections of spacing $\Omega\,\mathrm{d}t$ where each local flow velocity is calculated as by Kishida (1988) [6]. Equations 1 – 4 are then solved for each stream tube- section individually. As the time stepping progresses, the blades are rotated to the next stream tube section and the local velocities are re-calculated, thus accounting for the time variation of the flow.

*Corresponding author.
Email address: thomas.nevalainen@strath.ac.uk

Case study

A case study is presented where a TST is modelled in a moderate gale sea state to demonstrate the impact of wave and current loads. The parameters for the case are wave of height $H = 4$m following the flow, wave period $T = 7$s, turbine diameter $D = 10$m, current at sea bed $U_b = 1$m/s, current at surface $U_s = 2$m/s, depth $h = 30$m, hub height $h_{hub} = 15$meter, TSR = 5. At these conditions the mean power and thrust coefficients are $C_p = 0.38$ and $C_t = 0.63$. The scenario presented is illustrated in figure 1 and the blade loads are given in figure 2.

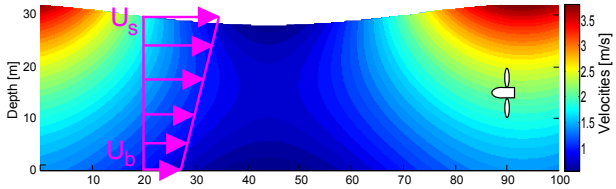

Figure 1: TST situated in rough weather site with shear current profile.

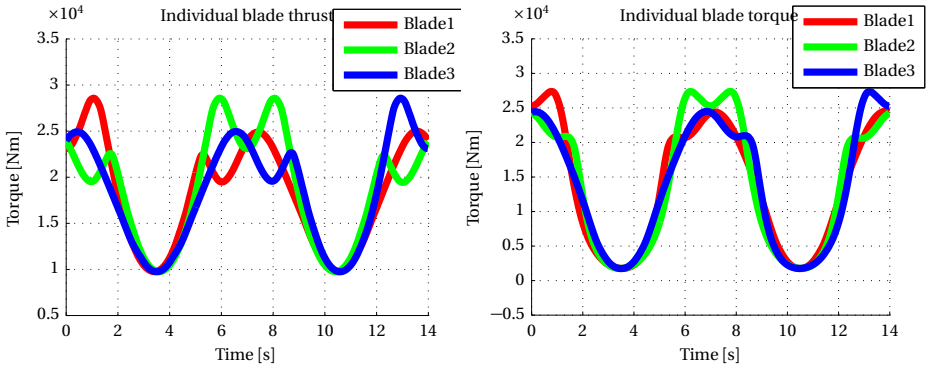

(a) Blade thrust forces

(b) Blade torque forces

Conclusions

It can be seen that the individual blade loads vary significantly during extreme sea conditions, fluctuating with as much as 2×10^4N, and that the loads across the blades also vary significantly in the radial direction (not pictured). This shows that there is a need for detailed fatigue analysis of TSTs in order to maximise their lifespan.

References:

[1] W. M. J. Batten, a. S. Bahaj, a. F. Molland, and J. R. Chaplin. The prediction of the hydrodynamic performance of marine current turbines. *Renewable Energy*, 33(5): 1085–1096, May 2008. ISSN 09601481. doi: 10.1016/j.renene.2007.05.043. URL `http://linkinghub.elsevier.com/retrieve/pii/S0960148107002133`.

[2] I A Milne, A H Day, R N Sharma, and R G J Flay. Blade loads on tidal turbines in planar oscillatory flow. *Ocean Engineering*, 60(0):163–174, 2013. ISSN 0029-8018. doi: http://dx.doi.org/10.1016/j.oceaneng.2012.12.027. URL `http://www.sciencedirect.com/science/article/pii/S0029801812004465`.

[3] C Swan, J P Cummins, and R L James. An experimental study of two-dimentional surface water waves propagating on depth-varying currents. Part 1. Regular waves. *Journal of Fluid Mechanics*, 428:273–304, 2001.

[4] T Wang and J Li. Effect of nonlinear wave-current interaction on flow fields and hydrodynamic forces. *Science in china*, 40(6), 1997.

[5] I. Masters and J A C Orme. A robust blade element momentum theory model for tidal stream turbines including tip and hub loss corrections. 10(1):25–36, 2011.

[6] N Kishida and Rodney J Sobey. Stokes theory for waves on a linear shear current. *Journal of engineering mechanics*, 114(8):1317–1334, 1989.

Synthetic Turbulence Generation for Turbine Modelling with BEMT

Michael Togneri, Ian Masters
School of Engineering, Swansea University, Swansea

Summary: This presentation examines methods of generating synthetic turbulence for use in blade element momentum theory simulations of tidal stream turbines. Two techniques are employed, both based on data gathered from field measurements. The first is a 'single-point' method, which generates a spatially-uniform but temporally-varying field, and the second is the synthetic eddy method (SEM) of Jarrin *et al*. [1,2], which generates a flowfield that varies in both space and time. This work is intended to help determine the best way to incorporate turbulence into BEMT models in order to capture its effects on turbine loads.

Methods

The single point method takes a large set of ADCP data, and for each bin of each beam breaks all the available data into several ten-minute subsets. From the spectra of these subsets, we determine average properties for each frequency and then randomly generate a synthetic spectrum based on these properties, which can be inversely transformed to obtain a synthetic time series for each bin. This can be repeated until the time series is as long as is desired.

This is a fairly straightforward procedure, but the principle drawback is that since the time series for each bin is generated individually, there is no correlation between neighbouring bins. Furthermore, since this effectively generates a synthetic ADCP record, we still have the usual problems of using an ADCP record i.e., we do not have a complete picture of the instantaneous velocity field at any point in space. To get a flowfield that is usable in a BEMT model we take a zero-averaged along-beam record and superimpose it on a mean longitudinal velocity to get a flowfield that varies in the longitudinal direction (equivalent to varying in time with the frozen turbulence hypothesis) but not in the lateral or vertical.

For the synthetic eddy method, we start by defining the region of space on which we want to generate a turbulent flowfield; for this study, this is taken to be the rotor plane. This is enclosed by a second, larger region we will call the 'eddy volume', a box whose limits are equal to those of the first region with the addition of a margin equal in size to the largest eddy we will simulate.

We generate N eddies to fill the eddy volume; eddy k has an associated position $\boldsymbol{x}^k$ and an intensity $\boldsymbol{c}^k$. The initial value of $\boldsymbol{x}^k$ is generated as a uniformly random point in the eddy volume. Each component of $\boldsymbol{c}^k$ is generated from the Cholesky decomposition of the Reynolds stress tensor, whose elements we denote a_{ij}, as $c_i^k = a_{ij}\varepsilon_j^k$ (using repeated index summation). ε_j^k here is a random variable whose value is distributed uniformly to ±1. With all positions and intensities defined, we can calculate each component of fluctuation velocity at a given point in space $\boldsymbol{x}$ by:

$$u_i'(\boldsymbol{x}) = \frac{1}{\sqrt{N}} \sum_{k=1}^{N} c_i^k f_\sigma(\boldsymbol{x} - \boldsymbol{x}^k)$$

f_σ is the shape function of the eddy, which is compactly supported on [-σ, σ] in all dimensions and is chosen such that its norm satisfies certain constraints. Once all eddies are generated and the resultant velocities evaluated for all desired points, we increment the time by convecting all eddies in the longitudinal direction according to the frozen turbulence hypothesis. Any eddies that are convected out of the downstream face box are recycled through the upstream face, with their lateral and vertical positions and ε_j^k-values randomly regenerated. With this scheme, we generate a turbulent flowfield whose autocorrelations and cross-correlations match the provided Reynolds stress tensor (or rather, would match for a simulation of infinite duration).

Sample results

In figure 1, we compare a real along-beam measurement with a synthetic one generated in a single-point fashion. It is clear that the behaviour of the synthetic data is very similar to that of the real data. When we extend this to bulk properties of the fluid, we see the same thing, as illustrated in the right-hand panel of figure 1 which

compares real TKE density profiles with one obtained from a synthetic ADCP data set generated in the manner described above. Figure 2 illustrates results obtained using the SEM method to generate a turbulent flowfield by comparing the input profiles of R11, R22 etc., with the resultant mean profiles from 25 different synthetic flowfields.

Acknowledgements:

This work was undertaken as part of the Low Carbon Research Institute Marine Consortium (www.lcrimarine.org.uk), and as part of SuperGen UK Centre for Marine Energy Research (UKCMER). The authors wish to acknowledge the financial support of the Welsh Assembly Government, the Higher Education Funding Council for Wales, the Welsh European Funding Office and the European Regional Development Fund Convergence Programme. The authors would also like to acknowledge the support of EPSRC through grant EP/J010200/1, which funds the UKCMER project.

References:

[1] Jarrin, N., Benhamadouche, S., Laurence, D., Prosser, R. (2006). A synthetic-eddy method for generating inflow conditions for large-eddy simulations. *Int. J. Heat and Fluid Flow*. **27** 585-593

[2] Jarrin, N. (2008). Synthetic Inflow Boundary Conditions for the Numerical Simulation of Turbulence. Ph.D. thesis, University of Manchester.

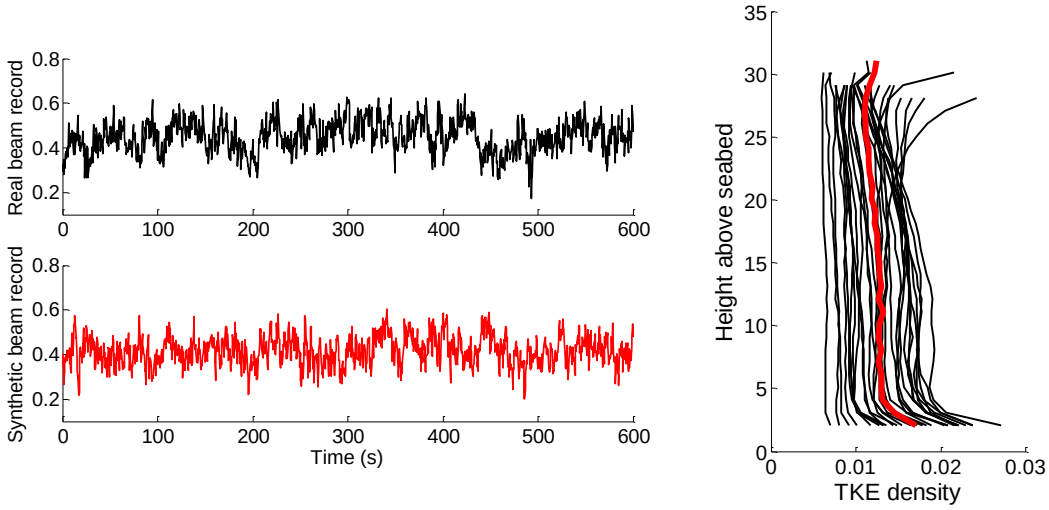

Fig. 1: Left-hand panel shows sample real along-beam velocity record (top, black) and sample synthetic record (bottom, red). Right-hand panel compares real TKE density profiles (black) with synthetic profile generated based on the same data. All real data taken from EMEC test site.

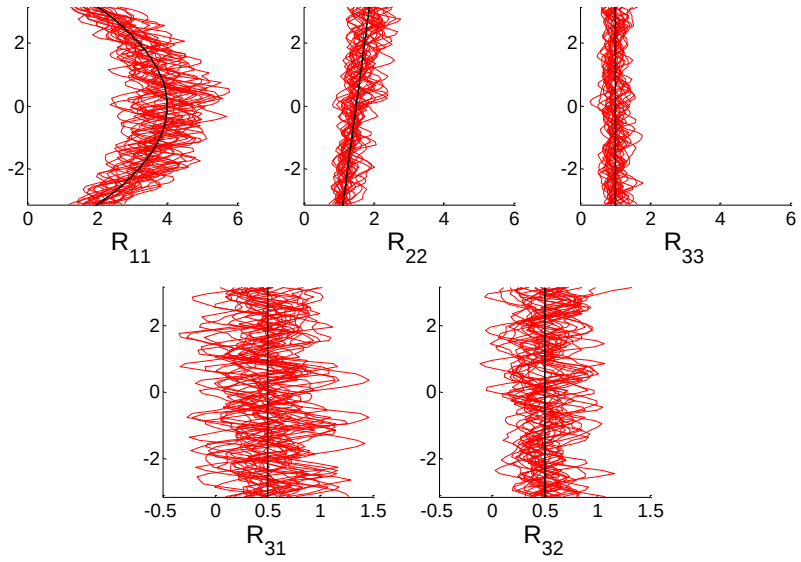

Fig. 2: Comparison of mean profiles of synthetic autocovariances and cross-covariances for 25 different flowfields (in red) generated using the SEM with the input covariance profiles (in black)

Wind and tidal turbines in uniform flow

Scott Draper
Centre of Offshore Foundation Systems, University of Western Australia, Australia

Takafumi Nishino, Thomas A. A. Adcock and Guy T. Houlsby
Department of Engineering Science, University of Oxford, UK

Summary: Estimating the power that can be extracted by wind or tidal turbines in uniform flow is complicated because the resistance offered by turbines acts to divert flow around them. In this paper we briefly review different models which can be used to understand this flow diversion. We start with Linear Momentum Actuator Disc Theory (LMADT), summarising some extensions that have been made in recent years to model more complex arrangements of turbines. We then consider some future extensions that could be made to LMADT and numerical approaches that complement LMADT. As an example of the latter we use a point vortex model to investigate (i) a non-concentrically placed actuator disc in a channel; and (ii) a V-formation of 5 discs.

Existing work on modelling turbines with actuator disc theory

Linear Momentum Actuator Disc Theory (LMADT) was used almost 100 years ago to model a single wind turbine as an actuator disc in laterally unbounded flow. Assuming the disc offered a streamwise resistance to the flow, arguments of mass, energy and momentum were used selectively to quantify the diversion of flow around the disc and the power extracted by the disc. This analysis led to the result that at most 16/27 times the upstream kinetic flux (passing through an area equal to that of the disc) can be extracted by the disc, which is often referred to as the Betz limit. In practice this limit has proven useful as a benchmark in the wind industry, whilst the combination of LMADT with blade element theory has provided a valuable wind turbine design tool [1].

Motivated by this success, a number of extensions to LMADT have been made in recent years. Most of these extensions have been introduced in the context of tidal stream turbines, and include: extensions to model isolated turbines in bounded flows; extensions to model rows of turbines; and extensions to model arrays of turbines. Beginning with isolated turbines, LMADT was initially extended to consider the performance of a tidal turbine placed in the middle of a uniform channel [2, 3]. This allowed the important effect of blockage ratio, defined as disc area to area of bounded flow, to be quantified (with the analytical results proving to be in reasonable agreement with later numerical simulations of turbines concentrically placed in a variety of channel shapes [4]). Following this work, theoretical extensions to LMADT considered the effect of a deforming flow boundary, which is a more correct representation for a tidal channel with a free surface [3, 5]. Collectively, this work on uniform and deforming bounded flows has allowed for the introduction of turbine efficiency as a metric to described turbine performance (defined as the power extracted by the disc to the total power removed from the flow). In many situations turbine efficiency is an equally important metric as the amount of power extraction (see [8] for further discussion). Moving beyond one disc and towards rows of discs, [6] has more recently introduced a concept of scale separation to consider partial fences of turbines placed within laterally unbounded or bounded flows. This work has provided, for the first time, a means to account collectively for flow diversion around individual turbines and around rows of turbines, and the theoretical model has been shown to agree well with CFD simulations of rows of up to 40 actuator discs [7]. Finally, stepping from rows of turbines towards arrays of turbines, the ideas of [6] have recently been combined with an assumption about streamwise spacing between discs to consider turbine farms comprised of staggered and multiple rows of discs [8]. This work is the first to suggest analytically that (i) staggering turbines may not be the most efficient means of farm layout in uni- or bi-directional flows, compared with placing turbines closely together in one single row, and (ii) that the optimal spanwise spacing between turbines placed in rows is strongly dependant on the size of the farm (i.e. how many rows of turbines).

Further modelling turbines as actuator discs

Each of the extensions to LMADT noted above have allowed for an increase in the complexity of problem that can be handled analytically. However, despite the number of extensions that have been made thus far, it is apparent that future extensions to LMADT are still possible. For example, [8] has shown that discs placed in non-uniform flow can be modelled using LMADT, and a dedicated study on turbines in sheared flows could be undertaken based on this. Extensions to the scale separation idea of [6] also appear likely, both for different farm layouts in channels, and for problems involving additional scales of separation. It may also be possible to learn more about the effect of turbine support structure on power extraction by introducing combined blockage and

drag in uniformly bounded flow. Finally extensions may be possible to treat the effects of different channel geometry and/or seabed drag on the power extraction of discs.

Aside from these theoretical possibilities, many important scenarios also exist in which turbines may be represented to first approximation as actuator discs (i.e. as discs introducing a uniform resistance) but LMADT cannot be used to quantify the flow field. Figure 1 and Figure 2 present two examples where this is the case: (i) a non-concentrically placed disc in a uniform channel and (ii) a V-formation of 5 actuator discs. These scenarios cannot be modelled with LMADT because in the first example LMADT is inherently one-dimensional and unable to consider geometric asymmetry, whilst in the second example LMADT can only be used to model multiple discs if the pressure equalises across the flow between successive discs [8].

To explore scenarios like those in Figure 1 and Figure 2 requires a numerical model. In this paper we adopt a point vortex model, described in [9] but adapted here to (i) model flow boundaries using the method of images (Figure 1) and (ii) model multiple discs (Figure 2). The vortex model has advantages over CFD because it is an efficient way to model inviscid flow, in keeping with traditional actuator disc approaches, and it allows naturally for the treatment of unbounded flow (when the method of images is not used). Using the vortex model Figure 1 illustrates how geometric asymmetry can be modelled (with results suggesting an increased power extraction). Figure 2 suggests that staggering leads to more variability in individual turbine power, but it does not increase total power generation. Each of these findings, which maintain the classic assumption that a turbine can be modelled as an actuator disc, suggests optimal strategies for arranging wind and tidal turbines in uniform flow.

Acknowledgements: The first author would like to thank the Lloyd's Register Foundation. Lloyd's Register Foundation helps to protect life and property by supporting engineering-related education, public engagement and the application of research. The second author would like to kindly acknowledge the Oxford Martin School.

References:

[1] Burton, T., Sharpe, D., Jenkins, N. & Bossanyi, E. (2001) *Wind Energy Handbook*. John Wiley & Sons, Ltd.
[2] Garrett, C. & Cummins, P. (2007) 'The efficiency of a turbine in a tidal channel', J. Fluid Mechanics, 588, 243-251.
[3] Houlsby, G. T., Draper, S. & Oldfield, M. L. G. (2008) 'Application of linear momentum actuator disc theory to open channel flow'. Tech. Rep. OUEL 2296/08. University of Oxford.
[4] Nishino, T. & Willden, R. H. J. (2012) 'Effects of 3-D channel blockage and turbulent wake mixing on the limit of power extraction by tidal turbines', International Journal of Heat and Fluid Flow, 37, 123-135
[5] Whelan, J. I., Graham, J. M. R. & Peiró, J. (2009) 'A free-surface and blockage correction for tidal turbines', J. Fluid Mech. 624, 281–291.
[6] Nishino, T. & Willden, R.H.J. (2012) 'The efficiency of an array of tidal turbines partially blocking a wide channel', J. Fluid Mech., 708, 596-606.
[7] Nishino, T. & Willden, R.H.J. (2013) 'Two-scale dynamics of flow past a partial cross-stream array of tidal turbines', J. Fluid Mech., 730, 220-244.
[8] Draper, S. & Nishino, T. (2014) 'Centred and Staggered arrangements of tidal turbines', J. Fluid Mech., 739, 72-93.
[9] Johnson, P. (2012) 'Hydrodynamics of tidal stream energy devices with two rows of blades', PhD Thesis, University College London.

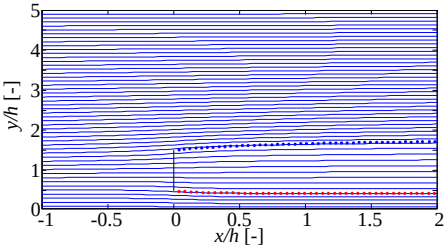

Fig.1 Disc with local resistance k =3.3 placed close to one side of a channel that is 5 times wider than the disc (k is a dimensionless thrust; see [8]). This disc removes more power than centring the turbine in the channel.

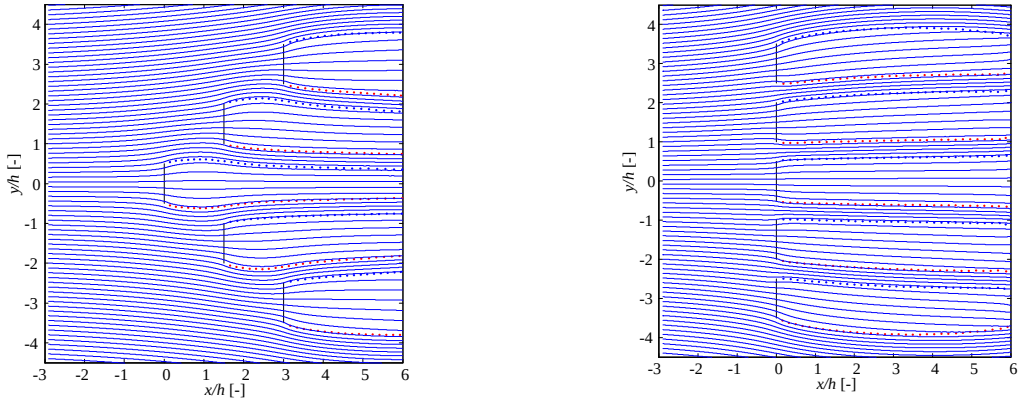

Fig. 2: (Left) 5 staggered discs each with k =2. From top, fraction of kinetic flux removed by disc, 1.03, 0.84, 0.6, 0.84, 1.03 (Right) Identical discs placed in a line. From top, fraction of kinetic flux removed by disc: 0.87, 0.88, 0.89, 0.88, 0.87.

The Potential of Sub-Arrays to Increase Tidal Farm Power

Susannah C. Cooke*, Richard H. J. Willden, Byron W. Byrne
Department of Engineering Science, University of Oxford, UK

Summary: Building on theoretical models previously developed for partial arrays of tidal turbines, a theoretical model has been developed to investigate the behaviour of a long fence array split into multiple shorter fences, or sub-arrays. Three flow scales are used for turbine, sub-array and channel flow, allowing the governing equations to be applied at each scale. Through varying blockage ratios, it is discovered that increasing the local blockage ratio, if over-blocked flow can be avoided, has the greatest potential to increase power yield. It is also found that splitting a sufficiently long fence array into sub-arrays can increase the power that can potentially be extracted.

Introduction

An analytical model for a single partial fence array of tidal turbines partially filling a wide channel has been previously developed by Nishino and Willden [1,2]. The previous work proposed a scale separation between the flow immediately surrounding each individual device and the flow around the complete array, with dynamic and kinematic matching between the two scales which allows an analytical solution to be found. The present work extends this concept of scale separation to a third scale, that around a 'sub-array'. This allows the investigation of a long row array that is split into multiple shorter arrays, which may be necessary or practical in reality where bathymetry is complex or where multiple devices are mounted on each support structure.

Methods

An analytical model of a tidal 'farm' including multiple sub-arrays was developed using Linear Momentum Actuator Disc Theory (LMADT). The basic model of a single turbine in a channel with constant mass flux was developed by Garrett and Cummins [3], who used LMADT to model the flow through and around a single turbine. This is a quasi-inviscid model, where wake expansion and pressure equalisation between the core flow and the bypass flow occur upstream of any mixing. This assumption allows the equations of conservation of mass, momentum and energy to be applied along the core flow and the bypass flow separately, and relationships between the thrust and power coefficients and the device induction factor can be found. The work of Nishino and Willden replaced the single device in this model with a partial fence array of devices, introducing the concept of separation of scales.

A multiple sub-array model has therefore been developed by extending this concept further, replacing each single device within the partial array model with a sub-array, such that there are three flow scales under consideration as shown in Fig. 1: the tidal farm scale, where a wide channel has a single 'device' within it, which is the entire tidal farm; the array scale, where multiple identical sub-array channels within the total farm contain single 'devices' within them, which are the sub-arrays; and the local scale, where each actual individual turbine sits in a local channel within its sub-array. The number of turbines and sub-arrays is considered to be high enough to justify the assumption of flow scale separation between each scale and the ones above/below it.

Kinematic matching between scales is ensured by equating the upstream flow speed at each scale to the 'device' location flow speed in the scale above it: i.e., the upstream flow speed in the turbine scale channel is equal to the sub-array's core flow speed at the array position. Dynamic matching between scales is simple, as the total thrust imposed on the flow by the total array must equal the sum of all the individual thrusts imposed by the turbines. These matching conditions allow the (numerical) solution of the system of governing equations at all scales if a local turbine induction factor is specified.

Results

The theoretical global power and thrust coefficients have been investigated over a parameter space representing a wide variety of different array configurations. Blockage ratios for the local, array and farm scale were defined as in Fig. 1 and varied independently, and for every blockage combination a range of local turbine induction factors were simulated to find the maximum power coefficient available. The case of fixed global blockage, B_G (which equals the product of the local, array and farm blockage ratios), was investigated in some

* Corresponding author.
Email address: susannah.cooke@eng.ox.ac.uk

detail, since it physically represents a channel with a fixed number of turbines of known area to be placed within it. For the case of $B_G = 0.131$, a maximum C_{PG} of 1.087 was found to be possible at $B_L = 0.65$, $B_A = 0.56$ and $B_F = 0.36$, as shown in Fig. 2a). This is 7.5% higher than the maximum C_{PG} of 1.011 achieved in the single partial array model of Nishino and Willden at the same global blockage, with $B_L = 0.49$ and $B_F = 0.27$. (B_A as defined in this model is equal to 1 in the single partial array model, as there is no separation between sub-arrays.) Basin efficiency (the ratio of extractable power to total power removed from the flow) was also investigated. As might be expected, basin efficiency, as shown in Fig. 2b), generally decreases in this model as extractable power is maximised, as this is accomplished through increased thrust. However, it should be noted that the lowest values of basin efficiency do not exactly correspond to the highest values of C_{PG}, so there is some opportunity to achieve a compromise solution between the two where required.

The order of blockage ratios in terms of their magnitude to achieve maximum C_{PG} as seen in this individual case, where $B_L > B_A > B_F$, was repeated at all global blockages considered within this analysis. Over the range of global blockages considered ($0 < B_G < 0.5$, which it is considered highly unlikely that any real tidal farm could ever exceed), it was also seen that the greatest increases in C_{PG} when moving from the single partial fence model to the multiple sub-array model were achievable at low global blockage. The specific case of $B_G = 0$ was considered, an infinite width channel that for tidal turbines is analogous to the wind turbine in free atmosphere, where C_{PGmax} takes the Lanchester-Betz limit of 0.593. For the multiple sub-array model, $C_{PGmax} = 0.865$ (an 8% increase on $C_{PGmax} = 0.798$ in the single partial fence case).

Conclusions

A new theoretical model has been proposed to investigate the efficiency of a long, cross-stream tidal farm, comprised of multiple sub-arrays partially filling a wide channel. This model is based on three scales of fluid flow; around the turbine, the sub-array and the entire tidal farm. The power coefficient for extractable power is found to be a function of the blockage ratios at all scales, and the flow speed induction factor through the turbine. It is found that the maximum power coefficient available can theoretically be increased above that achievable in the single turbine or single partial array models, though at some associated cost in basin efficiency.

Acknowledgements:

This work was done with the support of the SuperGen UK Centre for Marine Energy Research (UKCMER).

References:

[1] Nishino, T., Willden, R. H. J. (2012) *J. Fluid Mech.* **708**, 596-606.
[2] Nishino, T., Willden, R. H. J. (2013) *J. Fluid Mech.* **730**, 220-244.
[3] Garrett, C., Cummins, P. (2007) *J. Fluid Mech.* **508**, 243 -251.

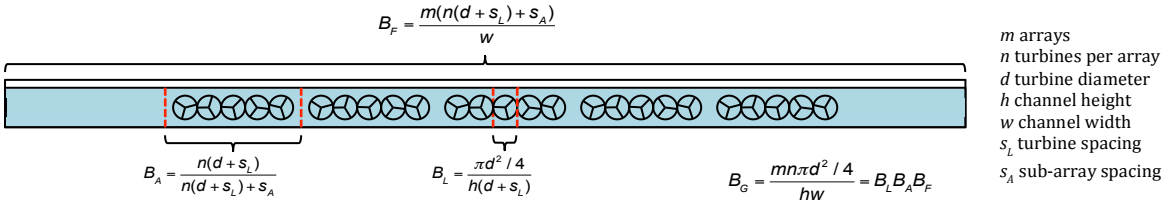

Figure 1 – An illustration of a tidal turbine farm containing multiple sub-arrays, with definitions of blockage ratios

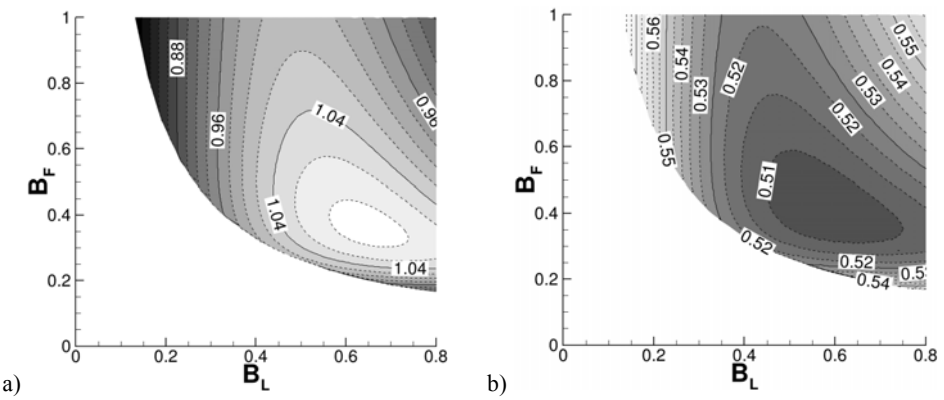

Figure 2 – Results for a) C_{PGmax} and b) η (basin efficiency) against B_L and B_F for the case of $B_G = 0.131$

Optimising the Number of Turbines in a Tidal Current Turbine Array

D. M. Culley[1], S.W. Funke, M. D. Piggott
Applied Modelling and Computation Group,
Department of Earth Science & Engineering,
Imperial College London, UK

Summary: Scenario specific physical, technological and practical considerations – among others – greatly impact upon both the appropriate number of turbines to include within a tidal current turbine array, and also the individual locations of those turbines. The latter has been shown to significantly impact upon the energy yield of an array [1] and thus in order to determine the power output of a given *number* of turbines, one must first optimise their arrangement on the proposed site. This leads to a nested optimisation approach. While this work is ongoing, preliminary findings have indicated that a practical approach to resource estimation of a given site requires a cost model combining both the increased power generated by additional turbines and the increased cost of those turbines. This model highlights a diminishing return on investment for developers of arrays consisting of more than the optimum number of turbines. This optimum number (and therefore the feasibly extractable resource of a given site) is highly scenario specific, depending on factors such as turbine design, the shape of the site leased for the farm and the assumed cost model for the development.

Introduction

It is well understood that assessing the accessible tidal current energy resource of a site, without taking into account the impact of the proposed turbines upon the flow, may overestimate the potential yield. Given turbine arrays can have such a significant impact upon the pre-existing flow, it follows that the presence of each turbine will impact strongly upon the operation of those surrounding it. Indeed this is the case, and it has been demonstrated that optimising the layout of individual turbines within an array - micrositing - facilitates increased energy harvest for a given number of turbines in a given area, as compared to a 'human's best attempt' design [1]. The optimal micrositing design of an array, and therefore an accurate forecast of the yield of that array, must be found as the product of an optimisation exercise which may incorporate turbine parameters, local bathymetry and a host of other practical, physical, legal, financial or environmental constraints. In general, as the number of turbines within the array increases, so the effects of that array on the flow and environment accumulate and objective measures (such as maximisation of energy yield or profit) begin to suffer the effects of diminishing returns. Consequently, determining the optimal number of turbines within an array proposed for a given site is a problem of critical importance and which also cannot be solved directly, but though a process of iterative optimisation. Optimising the number of turbines and their arrangement will help to provide a reliable estimate of the accessible tidal resource on a site.

Methods

Funke [1] proposed a method to optimise the micro-siting design of a tidal turbine array using the adjoint approach, this application is packaged in the open source code OpenTidalFarm [1]. The crux of the OpenTidalFarm methodology is the ability to efficiently determine the gradient of the functional of interest (Funke used the power output of the array) with respect to the locations of the turbines. Determining this gradient enables the use of efficient gradient-based optimisation algorithms which require far fewer iterations to find a solution. The efficiency with which the adoint approach finds this gradient and with which the gradient based optimisation finds a solution means that the underlying model can be more computationally demanding and therefore more characteristic of the real-world physics.

Determining the number of turbines for a given site involved firstly developing the existing OpenTidalFarm code so as to more fully parametrise the turbine representation (incorporating more accurate thrust and power curves) and secondly using OpenTidalFarm as a 'black box' and using a global optimisation strategy [2] in which each iteration represents a full optimisation run of OpenTidalFarm with a chosen number of turbines.

In this work, three scenarios are being considered; an idealised channel, an idealised channel with a central

[1] Corresponding author.
Email address: dmc13@imperial.ac.uk

island, and an approximation of the Inner Sound of the Pentland Firth. For each scenario, various different shapes and sizes of 'turbine area' are tested (i.e. the area leased by the developer in which turbines can be located - this captures practical considerations like the need to preserve shipping lanes past the array).

Results

While this topic is the subject of ongoing research, and the nature of the problem is highly scenario specific (bathymetric features, for example, on one site will lead to a different solution to that for a different site) some preliminary results for the case of the idealised channel have been found.

These initial observations imply that the power output of the array with number of turbines is convex, growing approximately linearly while turbines complete a 'fence' perpendicular to the flow, but beginning to plateau once spatial constraints prevent additional turbines from being incorporated into this row. The power output of the array eventually diminishes after a certain number of turbines are added. This number is highly sensitive to such scenario-specific conditions as the channel and turbine site dimensions, the flow regime of the undisturbed channel and the parametrisation of the turbines. It is clear from the data, however, that the average power output per turbine begins to suffer greatly before this maximum is met. Additionally the variance between the power generated by each turbine grows large as the upstream turbines are worked significantly harder than those sat in their wake.

Inclusion of a financial model helps to capture these issues, penalising both the addition of more turbines and designs in which the workload is not shared as equitably as possible among the turbines in the array. Ongoing work is aimed at fully developing this model and using it to maximise the return on investment as calculated by combining the array income; a function of the number of turbines and their locations and the development costs; a function of the number of turbines.

Conclusions

Preliminary results have demonstrated how critical determining the number of turbines in an array is, both to accurately calculate the available resource and to estimate the profit and cost of a proposed development. In physical terms, adding more turbines to a given site will yield more power, however the application of even a rudimentary cost model demonstrates that in business terms the array becomes cost ineffective long before that point.

This ongoing work will continue to evaluate idealised scenarios with real-world practical constraints such as lease areas and clear passages through the site for shipping. General conclusions from the results of these idealised scenarios will then be tested in representations of real sites. It seems likely that the shape and dimension of the turbine site relative to the prevailing flow directions will play a large part in determining the optimum number of turbines and therefore the magnitude of the exploitable resource.

References:

[1] Funke, S. W., Farrell, P. E., Piggott, M. D. (2014). Tidal turbine array optimisation using the adjoint approach. *Renewable Energy*, 63(0), 658-673.

[2] Jones, D. R., Schonlau, M., Welch, W. J. (1998). Efficient Global Optimization of Expensive Black-Box Functions. *Journal of Global Optimization,* 13(4), 455-492.

Tidal stream energy: designing for blockage

Richard H. J. Willden*, Takafumi Nishino, Justine Schluntz
Department of Engineering Science, University of Oxford, UK

Summary: The paper presents a new analytic model for the analysis of finite length turbine fences in channels driven by sinusoidally oscillating driving head. Thus the thrust presented by the turbines properly reduces the flow rate through the channel leading to a solution for overall power that is dependent upon blockage as well as channel characteristics. For a given channel, optimum, in terms of power per turbine, fence deployments can then be deduced. The model can be further extended to incorporate realistic turbine power and thrust curves.

Introduction

Significant advances have been made in recent years on the analytic modelling of tidal turbine arrays and farms. It is now well established that tidal turbines do not behave precisely as wind turbines and are subject to higher power extraction limits than the Betz limit due to the flow confinement effects (blockage) provided by the channel and neighbouring turbines. The work of Garrett & Cummins [1] set in place the upper energy extraction limit for a homogeneously arrayed turbine fence that completely spans the width of the channel under the assumption of an undeforming free surface. Later extensions by Whelan et al. [2] and Vennell [3] allowed respectively for the deformation of the free surface and the response of the channel flow rate to the resistance presented by the turbines. Later work by Nishino & Willden [4] extended the model of Garrett & Cummins to consider the practical case of a long but finite length turbine fence partially spanning the width of a channel; hereafter referred to as the NW12 model. This model, working on the basis of scale separation between turbine and array scale flow events, led to the development of an energy extraction limit for a closely packed turbine fence in an infinitely wide channel of 79.8% of the kinetic energy in the undisturbed approach stream, achieved at a local blockage (ratio of turbine to local flow passage area) of 0.4.

Whilst these models have made significant advances they are still a long way short of representing a realistic turbine installation, even in a simplified analytic sense. Whilst the NW12 model allows for finite length fences, and thus incomplete channel usage as will be required for shipping lanes, bathymetric variations etc., it is restricted to a constant flow rate through the channel, i.e. the channel is unresponsive to the resistance presented by the turbines. Further, all of the models discussed above are for actuator disk representations of turbines that are able to extract energy at will, in an optimal fashion, from the flow by presenting it with an ever increasing resistance. Real turbines will be subject to power capping, which changes the relationship between flow speed and turbine thrust. Moreover, whilst the analytic models tell us that higher power limits can be obtained if high thrust can be imposed they say nothing about whether these high thrusts can be achieved in practice.

This paper presents a new analytic model that embeds the multi-scale finite fence model of NW12 in the channel dynamics model of Garret & Cummins [5] (GC05). A further development of this model sees the local turbine actuator disk model replaced by local blockage corrected power and thrust characteristics for a realistic turbine. The resulting model enables a finite length fence of turbines partially spanning a wide head driven channel to be analysed. Finally, we will, in the presentation, address the issue of whether turbines can be designed to present increased thrust and take advantage of the local blocking effects.

Finite Fence Channel Dynamics Model

The one-dimensional channel dynamics model of GC05 can be cast in non-dimensional form:

$$\frac{dQ'}{dt'} - \cos t' = -\frac{1}{2}Q'|Q'|\left(\frac{\sqrt{ag}}{\omega L}\right)^2\left(B_A C_{TA} + C_f \frac{L}{h}\right) \tag{1}$$

in which the flow is driven through the (here presumed) rectangular cross-section channel, length L, width w, height h, by a sinusoidally varying head difference between the ends of the channel, amplitude a frequency ω. $Q' = Q/Q_0$ is non-dimensional flow rate, in which Q_0 is the peak flow rate in the undisturbed channel, $t' = \omega t$ is non-dimensional time. The resistance to the flow has two contributions; from bed friction, included through the friction coefficient, C_f, and due to turbine array thrust, included through the array thrust coefficient $C_{TA} = T_A / \frac{1}{2}\rho U^2 w_A h$, in which T_A and $U = Q/wh$ are the array thrust and velocity, w_A the width of the array.

* Corresponding author. *Email address*: richard.willden@eng.ox.ac.uk

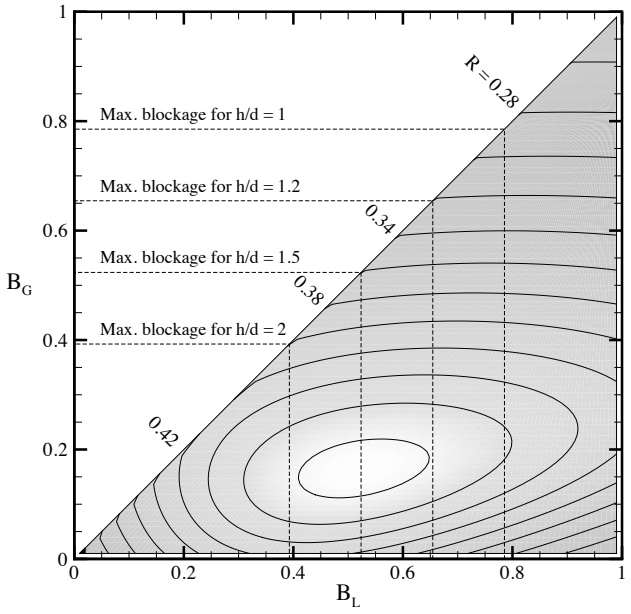

Fig. 1: Return parameter, $R = C_{PC} / B_G$, over local and global blockage space for channel parameters $\omega L / \sqrt{ag} = 0.635$, $L/h = 500$ & $C_f = 0$. Dashed lines indicate achievable blockages for given depth to turbine diameter ratios, h/d.

The array blockage ratio $B_A = w_A / w = B_G / B_L$ represents the proportion of the channel width occupied by the fence, whilst the local and global blockage ratios, B_L and B_G, the proportions of the local flow passage area and channel area occupied by turbines. The model assumes a smooth entry and exit to the channel and is closed through the specification of C_{TA} from the partial fence model of NW12.

Fig. 1 presents example solution to the finite fence channel dynamics model for given channel parameters in terms of the return parameter, $R = C_{PC} / B_G$; the ratio of power generated to turbine frontal area (note $C_{PC} = \overline{P} / \rho g a Q_0$ is the channel power coefficient and $\overline{P}$ the time average power generated). The local blockage infers the intra-turbine spacing so that for fixed B_L, increasing B_G corresponds to increasing the number of turbines and therefore length of the turbine fence. Increasing global blockage in this manner is seen to at first increase R, and thus power per turbine, due to the effect of restricting the array by-pass, but further increasing the fence length leads to a reduction in R through reduction in channel flow rate, although total power yield C_{PC} does continue to increase in this case (not shown here). There clearly exists an optimum point of operation if the desired outcome is to maximize power yield per turbine as opposed to total power yield.

Conclusions

To fully model the energy extraction by a tidal fence it is clearly necessary to consider the dynamics of the channel as the overall flow resistance plays an important role in limiting the potential power yield of the fence. Optimum points of operation (maximum yield per turbine) can be determined using this relatively simple finite fence channel dynamics model. Inclusion of realistic turbine thrust and power characteristics, as well as support structure drag and bed friction leads to more complex solution and will be presented at the workshop. Performance of real turbines to achieve high thrust singularly and in fence configuration will also be presented.

Acknowledgements:

The authors would like to thank the Oxford Martin School and the Rhodes Trust for supporting this research.

References:

[1] Garrett, C. & Cummins, P. (2007). The efficiency of a turbine in a tidal channel. *J. Fluid Mech.* **588**, 243-251**.**

[2] Whelan, J., Graham, J.M.R. & Peiró, J. (2009). A free-surface and blockage correction for tidal turbines. *J. Fluid Mech.* **624**, 281-291.

[3] Vennell, R. (2010). Tuning turbines in a tidal channel. *J. Fluid Mech.* **663**, 253-267.

[4] Nishino, T. & Willden, R.H.J. (2012). The efficiency of an array of tidal turbines partially blocking a wide channel. *J. Fluid Mech.* **708**, 596-606.

[5] Garrett, C. & Cummins, P. (2005). The power potential of tidal currents in channels. *Proc. R. Soc. A* **461**, 2563-2572.

Tidal Stream Turbine Modelling in the Natural Environment

Alison J. Williams, Matt Edmunds*, Ian Masters, T. Nick Croft.
MERG, College of Engineering, Swansea University, UK

Summary: Tidal stream renewable energy is becoming a viable source of electricity as part of a diversified low carbon energy mix. Across the world sites are being identified where the currents are sufficiently strong to enable economically attractive levels of energy extraction. Academic interest in the sector is growing in parallel to the growth of industrial investment. A large number of papers have now been published, ranging from device design, through environmental impact, to the hydrodynamic performance of devices, individually and in arrays. It is one of the remaining issues that this work seeks to inform. Inspired by Draper et. al. [1], marine currents around a headland are modelled with a single row fence of turbines placed offshore from the headland at various blockage ratios. Power performance estimates and downstream wakes are created showing increased power per device, and improved total power production as the blockage ratio rises from 0.13 to 0.20. This work uses a RANS computational fluid dynamics model with an embedded blade element actuator disk, described in [2], to investigate various aspects of this problem.

Introduction

To understand the effect of placing arrays of marine turbines close to a headland, it is useful to study the flow blockage caused by these turbines. Draper et. al. [1] demonstrate a method for predicting potential power extraction over a full tidal cycle using a method similar to the classic actuator disc model expressed over a lateral fence. The fence is situated off the tip of the headland at a location capturing the maximum kinetic flux within the domain. The authors perform their simulations utilising a 2D mesh representing a depth averaged domain. Described in their work is the blockage ratio; the ratio of turbine area and channel area confined to the pitch of turbines in the lateral fence array. In our work we study the effects on flow within a 3D domain using the BEM-CFD model to determine if the characteristics observed in [1] are comparable. The method is described in, and applied to arrays in [3]. Our study uses a turbine of diameter $10m$ situated in a $30m$ uniform depth channel at a location consistent with [1]. The rotors operate at a TSR of 3.0, i.e. $2.32 - 2.62rad/s$. It is a trivial extension to consider depth variation. For our simulations we use blockage ratios of 0.13, 0.17, and 0.20. This provides a more realistic density of devices for our study as we do not simulate the sloping bathymetry of the coastline. In summary the mesh resolution of the blade region is a structured grid at 0.2m resolution orthogonal to the flow, and 0.1m in the flow direction. The area around the blade has an unstructured resolution of 0.5m. The near wake and upstream region is 1.0m. The far wake region is 2.0m, and the remaining domain is 4.0m maximum resolution.

Results

In general, the lateral fence compares with the trends observed in the work by Nishino et. al. [4]. However, differences occur in the near/far wake regions due to rotor and nacelle influenced wake structure variations, and the influence of the headland on the general flow variation across the fence. The headland study highlights some useful phenomena related to deployment of arrays in realistic channels. Although the case has one simple variation to a uniform cross section, the presence of the headland and the close spacing of the rotors leads to a number of flow features. The performance variation of the rotors is consistent with the velocity variation, and the results do show positive blockage leading to higher power output. The effect of the fence on the flow are also seen with the increased velocity of the bypass flow and the curved nature of the downstream wakes. The fence location of the headland is consistent with [1] who target the area of maximum kinetic flux over a tidal cycle. However the kinetic flux is computed with reference to a sloping bathymetry around the coastline, thus moving the location seaward. In our study we notice that the maximum power extraction increases significantly towards the coast, see Figure 1. This is due, in our model, to the area of maximum kinetic flux being located at the coastline of the headland. This is the result of modelling different bathymetry along the coastline. The recirculation downstream of the headland can be seen clearly in Figure 2 for all four cases. The most noticeable difference is between the baseline case and the three fence cases. The flow separation for the baseline case is located further around the headland. In comparison to the fence cases, the velocity is significantly less and the rotation of the flow is elongated along the coast.

*Corresponding author.
Email address: m.edmunds@swansea.ac.uk

The addition of the turbine fence may have an impact on the local environment, in particular the sediment transport system. The characteristic increase in ocean flow and reduction in headland bypass flow, due to the fence blockage, is consistent with the findings of [1].

Conclusions

There are a number of papers which examine different aspects of marine turbines providing new knowledge for the industry supporting successful deployment of arrays in differing ocean topographies. Our work further extends the current published works. In the headland case the general trend of flow characteristics is in line with [1]. However, positioning of an optimal fence turbine array is very dependant on the local bathymetry close to the headland/coastline. This also effects the optimum fence packing density in this area maximising power extraction. It is likely that the combination of local bathymetry, avoidance of hazards to shipping, and environmental mitigation will restrict developers ability to place turbines in optimal locations. Finally, we conclude that these simulations of tidal turbine array design will, in a small way, help the progress of marine renewable energy.

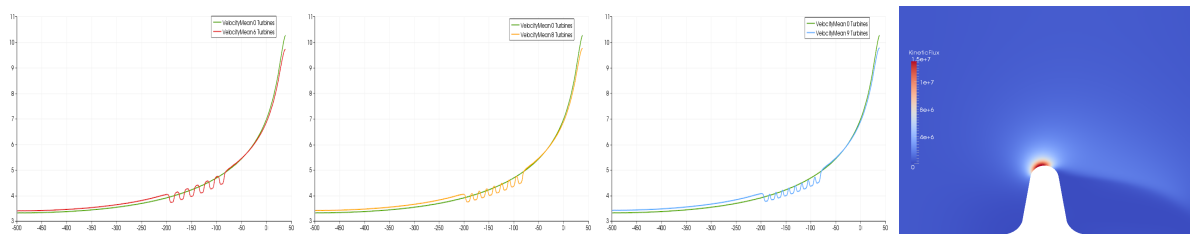

Figure 1: A comparison of depth averaged velocity profiles for different blockage ratios of tidal fences. A baseline depth averaged velocity profile without a tidal fence is shown in all three graphics. Fence blockage ratios of 0.13, 0.17, and 0.20 are equivalent to 6, 8, and 9 turbines respectively. The Kinetic Flux is defined as $0.5\rho|u|^3h$ where u is the local velocity, ρ is density, and h is the local channel depth.

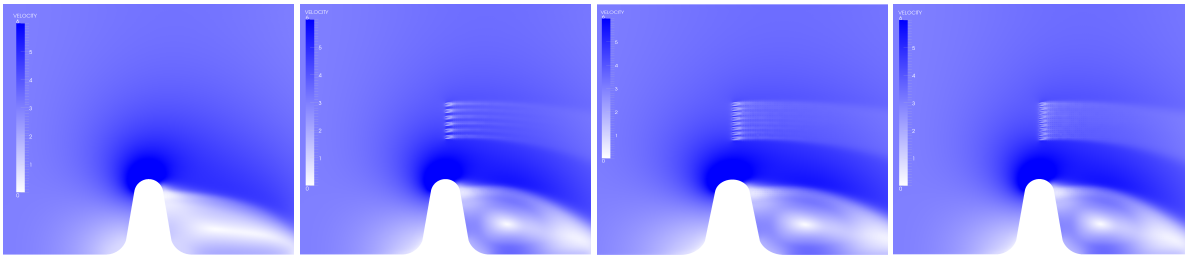

Figure 2: A comparison of the four headland cases from left to right; no turbine fence (baseline condition), turbine fence blockage ratio 0.13 (6 rotors), turbine fence blockage ratio 0.17 (8 rotors), and turbine fence blockage ratio 0.20 (9 rotors). The images illustrate a velocity magnitude slice at rotor centre depth.

Acknowledgements:

This work is undertaken as part of the Low Carbon Research Institute Marine Consortium (www.lcrimarine.org). The authors wish to acknowledge the financial support of the Welsh Assembly Government, the Higher Education Funding Council for Wales, the Welsh European Funding Office, and the European Regional Development Fund Convergence Programme.

References:

[1] S Draper, AGL Borthwick, and GT Houlsby. Energy potential of a tidal fence deployed near a coastal headland. *Philosophical Transactions of the Royal Society A*, 371(1985), 2013.

[2] R Malki, AJ Williams, TN Croft, M Togneri, and I Masters. A coupled blade element momentum–computational fluid dynamics model for evaluating tidal stream turbine performance. *AMM*, 37(5), 2013.

[3] Rami Malki, Ian Masters, Alison J Williams, and T Nick Croft. Planning tidal stream turbine array layouts using a coupled blade element momentum–computational fluid dynamics model. *Renewable Energy*, 63, 2014.

[4] T. Nishino and R.H.J. Willden. Two-scale dynamics of flow past a partial cross-stream array of tidal turbines. *Journal of Fluid Mechanics*, pages 220–244, 2013.

The power potential of a tidal turbine array with turbine power capping

Christopher R. Vogel*, Richard H. J. Willden, Guy T. Houlsby
Department of Engineering Science, University of Oxford, UK

Summary: The fluctuating nature of the tidal resource means that it is not economical to design turbines to extract the maximum power during peak tide, so turbines will be limited to a more economical rated power. The impacts of such power capping have thus far not been well understood. This paper combines Blade Element Momentum theory with Linear Momentum Actuator Disc Theory derived for tidal turbines to determine the effect of power capping on the power of a tidal turbine array. It is found that the effect of increasing blockage, the ratio of the swept rotor area to the cross-sectional area of the surrounding flow passage, is to cause the turbine to spin more slowly and reach power capping at a lower upstream flow speed than unblocked turbines.

Introduction

It is recognised that significantly harnessing the global tidal resource will require the deployment of many turbines in an array configuration; one estimate for extracting 1.9GW from the Pentland Firth in the UK requires thousands of turbines [1]. Analytical and numerical methods have been developed to model the large arrays of turbines required to extract this power. One key result is that there is a scale separation between array-scale flow events and turbine-scale flow events [2, 3]. Analytical models provide a useful basis to understand the dynamics of the flow around an array of turbines, but they are restricted to idealised parameters to represent the turbines.

Some of these short-comings can be overcome with numerical techniques, such as depth-averaged simulations, to capture more complex flow features; multi-scale flow, shear, etc. Although numerical simulations offer an improved method for determining the power potential of a turbine array, correctly representing the turbines to capture the core and bypass flows requires careful implementation. One method of implementing this is to use a sub-grid scale actuator disc model [4, 5].

Although depth-averaged simulations provide a means to determine an upper bound on the extractable power of a turbine array, it is often (as in actuator disc type studies) assumed power extraction is proportional to the cube of the velocity. This may be reasonable at lower flow speeds, but becomes unrealistic at higher flow speeds as turbines will be limited to a maximum rated power, due to constraints such as generator capacity. Capping at higher flow speeds means that the turbine characteristic departs from the cubic relationship with flow velocity, and thus the flow dynamics around the turbines and the array will be altered. This paper introduces a power capping methodology into the depth-averaged simulation framework, allowing real turbine data to be used to parameterise the turbines and providing a more realistic upper bound to the extractable power potential of a turbine array.

Methods

Figure 1 shows a plan view of a long turbine array partially spanning a wide channel. There are two scales of flow; the array-scale flow, which scales on the size of the array and evolves slowly, and the turbine-scale flow, which scales on the size of the turbine and evolves much more quickly. The flow velocity through the array, u_a, is the upstream velocity boundary condition to the turbine-scale problem. The thrust applied by the turbine to the flow is a function of the velocity through the device, u_d, and the rated power, P_R. P_R is specified as an operating parameter of the turbine, as is the 'rated velocity', u_r, at which rated power is achieved.

The thrust applied by the turbine on the flow is determined using Blade Element Momentum (BEM) theory, which is coupled with the Linear Momentum Actuator Disc Theory (LMADT) for a turbine in a channel with a rigid lid proposed by Garrett and Cummins [6]. This represents a novel coupling between momentum theory for flow around a turbine and the BEM theory. Critically, it allows blockage, the ratio of the swept area of the turbine rotors to the cross-sectional area of the flow passage surrounding the turbine, which strongly affects power potential of a tidal turbine, as shown by Garrett and Cummins and others, to be accounted for.

Given rotor geometry and blade parameters, lift and drag coefficients, C_l and C_d respectively, the velocity induction factor in turbine wake, relative the far upstream flow speed, $a_4 = 1 - u_4/u_a$ is:

$$a_4 = \frac{\sigma(1-a_2)^2(C_l\cos\phi - C_d\sin\phi) - b_4(2+b_4)\sin^2\varphi}{2(1-a_2)\sin^2\phi}; \quad a_2 = 1 - \frac{u_d}{u_a}; b_4 = 1 - \frac{u_b}{u_a} \tag{1}$$

* Corresponding author
Email address: christopher.vogel@eng.ox.ac.uk

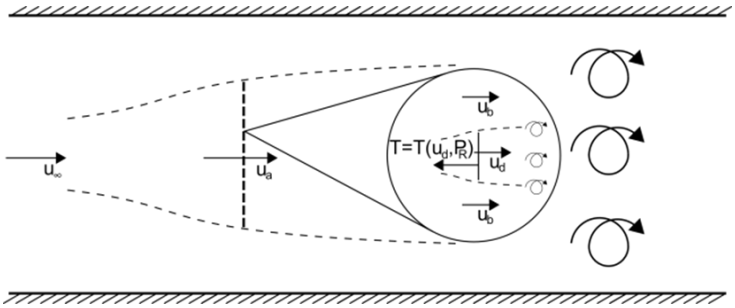

Figure 1: Plan view of a large turbine array, with inset showing flow around individual turbine

where a_2 is the turbine velocity and b_4 the bypass velocity normalised by the upstream velocity, φ is the angle between the plane of rotation and the relative velocity vector, and σ is the solidity of the rotor. If the radius of the blade element is r, the induced rotational velocity a' is calculated as:

$$a' = \frac{\sigma(C_l \sin\phi - C_d \cos\phi)}{4sin\varphi cos\varphi - \sigma(C_l \sin\phi - C_d \cos\phi)} \quad (2)$$

An iterative solution method is used where an initial value for α_2, α_4, and a' are assumed, based on an unblocked rotor, and the velocity in the axial and tangential directions of the plane of rotation are calculated. The lift and drag forces are calculated based on the lift and drag coefficients for the aerofoil being used, which is then used to update the estimates for α_2, α_4, and a'. This is repeated iteratively until converged. The blocked turbine thrust and power are then calculated and power capping implemented when rated power is reached. The thrust/power relationship is then applied to turbine arrays in shallow water numerical models, which shall be presented in the workshop.

Conclusions

The theory described above has been applied to a turbine with the NREL S809 aerofoil section. It is found that the turbine blockage ratio plays an important role in the dynamics of turbine power capping. One effect of increasing the blockage of a turbine is that the velocity through the turbine is increased relative to that in an unblocked condition. Keeping the thrust of the turbine equal, a higher blockage turbine rotates more slowly than a lower blockage turbine. In addition to this, turbines in higher blockage reach power capping operation at a lower upstream velocity (u_a in figure 1). This may be beneficial to the economics of deploying turbines in arrays of many turbines where the inter-turbine spacing is kept low.

The role of power capping may be particularly important when tidal dynamics are considered in the context of a tidal channel or basin, as power capping will be in effect for only a portion of the tidal cycle, and will play an important role in determining what an economically and technically feasible power capping limit P_R should be set for the turbines. This is the subject of ongoing investigation.

Acknowledgements:

The authors would like to acknowledge the support of the Oxford Martin School, University of Oxford, for funding this research.

References:

[1] Adcock, T. A. A., Draper, S., Houlsby, G.T., Borthwick, A. G. L, and Serhadlıoğlu, S. "The available power from tidal stream turbines in the Pentland Firth" *Proceedings of the Royal Society A*, **469** (2157), 2013
[2] Nishino, T. and Willden, R. H. J. "The efficiency of an array of tidal turbines partially blocking a wide channel", *Journal of Fluid Mechanics*, **708**, 2012, pp. 596-606
[3] Vogel, C. R., Houlsby, G. T., and Willden, R. H. J. "The extractable power of a turbine array spanning a wide channel" *Submitted* (*Journal of Fluid Mechanics)*, 2014
[4] Draper, S. "*Tidal stream energy extraction in coastal basins*" DPhil Thesis, University of Oxford, 2011
[5] Vogel, C. R., Willden, R. H. J., and Houlsby, G. T. "A correction for depth-averaged simulations of tidal turbine arrays" *To be submitted*, 2014
[6] Garrett, C. and Cummins, P. "The efficiency of a turbine in a tidal channel" *Journal of Fluid Mechanics*, **588**, 2007, pp. 243-251

Tidal resource characterization at a strait between an island and a semi-infinite landmass

Alberto Pérez-Ortiz[*1], Alistair Borthwick[2], James McNaughton[3], Paul Vigars[3]
[1]*Industrial Doctoral Centre for Offshore Renewable Energy, The University of Edinburgh, UK*
[2]*Institute of Energy Systems, School of Engineering, The University of Edinburgh, UK*
[3]*Alstom Ocean Energy, Bristol, UK*

Summary: Many sites where tidal energy may be exploited can be modelled as a strait between an island and a semi-infinite landmass. The presence of the island constrains the flow and induces a local acceleration in the current that yields high energy densities in the strait. This presentation will describe a preliminary study that is on-going into the influence of the strait and island geometry and the seabed friction on tidal power extraction from the strait. The length of the strait, width of the island, and seabed drag are anticipated to have a positive correlation with the ratio of maximum dissipated power to the undisturbed kinetic energy flux in the strait.

Introduction

As the tidal energy industry progresses towards the construction of the first commercial arrays, increasingly accurate understanding of the available tidal resource is needed. There are currently two main approaches to tidal resource assessment. The first uses a combination of theoretical and numerical models to assess energy extraction in idealised coastal geometries [1]. The second applies numerical models to simulate tidal currents and the consequent hydrodynamic effects from energy extraction at real coastal sites [2]. Furthermore, the findings from the first approach are useful for verification of models under development using the second approach.

Coastal geometries such as the channel between two infinite basins have been analysed extensively for tidal energy exploitation. The extractable resource from a channel has been characterized using one-dimensional analytical models [3] and for more complex two-dimensional models by the numerical solution of the shallow water equations [4]. In addition, other coastal geometries of interest to tidal energy such as oscillating bays and headlands have also been investigated [5]. An important number of tidal energy projects may be developed in coastal sites defined by a strait between an island and a semi-infinite landmass. The present work aims to increase the understanding of this coastal geometry and identify the key parameters driving the energy resource available at the strait.

Computational method

This study will be carried out solving the non-conservative form of the shallow water equations (SWE) using the finite element numerical code Fluidity-ICOM [6].

Fig. 1 presents the proposed model set-up and outlines the geometry parameters considered for the analysis. An island in the vicinity of a semi-infinite landmass is located at the south part of the domain. The semi-infinite landmass, island and northern boundary are defined using slip conditions. Open conditions are applied at the east and west boundaries of the model. The geometry of the model is defined by a characteristic domain length L, domain width B and mean water depth h. For each island and tidal farm setup, an analysis of the model length is carried out to investigate the sensitivity of the open boundaries to wake effects or long wave reflections from the internal flow obstacle(s). Likewise, the selected model width ensures that a free-stream current velocity u_{fs} is relatively undisturbed to the north of the island. The geometry of the island is elliptical, and it is defined by its length L_i and width B_i. The distance between island and landmass define the width of the strait s, where u_o refers to the current velocity at the strait.

A quasi-steady analysis is undertaken with constant water head drop ($h_w - h_e$) set from west to east of the domain. The head drop is established to yield a desired current velocity in the strait in the absence of power extraction by turbines. Seabed energy dissipation is parameterised using a dimensionless friction coefficient C_f. A range of C_f is considered that agrees with published numerical models of real coastal sites [7].

Energy extraction is implemented in the model through the addition of a turbine stress term in the momentum equations based on the turbine thrust and structural drag smeared across a grid element [8]. The turbine stress term that accounts for the tidal farm is modelled following the methodology described by Plew and Stevens [9], whereby the turbine stress term is evaluated for N turbine, with each turbine is defined by its rotor swept area

[*] Alberto Pérez Ortiz.
Email address: alberto.perez.ortiz@ed.ac.uk

(A_T), support structure area (A_S), and thrust and drag curves. This permits different types of turbine arrangements within the farm, noting the restriction that the momentum effect of turbines is assumed uniform across each mesh element. Mesh refinement could help reduce this drawback. The tidal farm has a width B_f equal to the width of the strait and it is located at the centre of the strait (Fig. 1). The length of the farm L_f is based on the chosen mesh edge length at the strait and typical downstream length scale of a staggered two row tidal array.

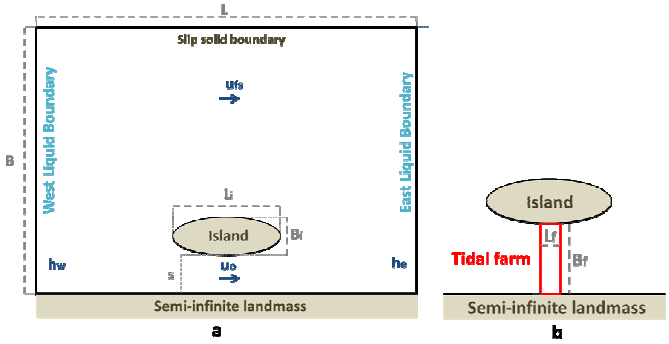

Fig. 1. Strait between an island and a semi-infinite landmass, a) model geometry and tidal parameters; and b) geometry of the tidal farm

Anticipated Results

The ratio of maximum dissipated power to the undisturbed kinetic flux at the strait is analysed for a set of different geometrical parameters and seabed friction coefficients. Although no conclusive results are yet available, a positive correlation between this ratio and length and seabed friction of the strait is expected. Increases in the length of the island and/or seabed friction imply larger impedance to flow in the strait and so the contribution from tidal farm to the total impedance of the strait is lower in relative terms. An increase in the width of the island means higher impedance for the flow bypassing the island, and thus should correlate favourably with the ratio of maximum dissipated power to the undisturbed kinetic flux at the strait.

Conclusions

This study analyses the ratio of maximum dissipated power to the undisturbed kinetic flux at the strait between an island and a semi-infinite landmass for a set of geometry parameters. The ratio is expected to correlate positively with the length of the strait, width of the island and seabed drag.

Acknowledgements:

The authors would like to thank Alstom Ocean Energy and IDCORE for their support.

References:

[1] I. G. Bryden and S. J. Couch, “ME1—marine energy extraction: tidal resource analysis,” *Renew. Energy*, vol. 31, no. 2, pp. 133–139, Feb. 2006.

[2] S. Serhadlıoğlu, T. A. Adcock, G. T. Houlsby, S. Draper, and A. G. L. Borthwick, “Tidal stream energy resource assessment of the Anglesey Skerries,” in *European Wave and Tidal Energy Conference*, 2013.

[3] C. Garrett and P. Cummins, “The power potential of tidal currents in channels,” *Proc. R. Soc. A Math. Phys. Eng. Sci.*, vol. 461, no. 2060, pp. 2563–2572, Aug. 2005.

[4] S. Draper, “Tidal stream energy extraction in coastal basins,” *Univ. Oxford, DPhil Thesis*, p. 253, 2011.

[5] S. Draper, A. G. L. Borthwick, and G. T. Houlsby, “Energy potential of a tidal fence deployed near a coastal headland Energy potential of a tidal fence deployed near a coastal headland,” *Philos. Trans. R. Soc. A Math. Phys. Eng. Sci.*, vol. 371, no. January, 2013.

[6] C. J. Cotter, D. a. Ham, and C. C. Pain, “A mixed discontinuous/continuous finite element pair for shallow-water ocean modelling,” *Ocean Model.*, vol. 26, no. 1–2, pp. 86–90, Jan. 2009.

[7] S. Baston and R. Harris, “Modelling the Hydrodynamic Characteristics of Tidal Flow in the Pentland Firth,” *Proc. Eur. Wave Tidal Energy Conf. No. 317*, 2011.

[8] A. Pérez-Ortiz, J. Pescatore, and I. Bryden, “A Systematic Approach to Undertake Tidal Energy Resource Assessment with Telemac-2D,” in *European Wave and Tidal Energy Conference*, 2013.

[9] D. R. Plew and C. L. Stevens, “Numerical modelling of the effect of turbines on currents in a tidal channel – Tory Channel, New Zealand,” *Renew. Energy*, vol. 57, pp. 269–282, Sep. 2013.

A 3D model of asymmetry in the Orkney tidal energy resource

Simon P. Neill*, M. Reza Hashemi, Matt J. Lewis
School of Ocean Sciences, Bangor University, UK

Summary: One factor that is not routinely considered in tidal energy site selection, yet which has an important role in quantifying the resource, is tidal asymmetry. Here, we present theory and develop a high-resolution 3D ROMS tidal model of Orkney to examine net power output for a range of sites along an energetic channel which exhibits varying degrees of tidal asymmetry. Since power output is related to velocity cubed, even small asymmetries in velocity lead to substantial asymmetries in power output. We also use the 3D model to assess how tidal asymmetry changes with height above the bed, i.e. representing different device hub heights, how asymmetry affects turbulence properties, and how asymmetry is influenced by wind-driven currents.

Introduction

From a resource and device perspective, it is clearly beneficial to select tidal energy sites where the tidal currents have an equal magnitude between the flood and ebb phases of the tide (tidal symmetry), and less desirable to exploit sites which have either strong flood- or ebb-dominance (tidal asymmetry). Tidal asymmetry not only affects the primary variables of the flow field such as velocity and water elevation – it is also expected to cause asymmetry in turbulence properties such as Reynolds stresses and turbulent kinetic energy, important variables in site selection [1].

Tidal waves are progressively distorted and dampened as they propagate in shallow-water coastal regions [2]. Although tidal waves in such regions still satisfy the criteria of long waves (i.e. wavelength is much greater than water depth), in shallow water the amplitudes of the waves become a significant fraction of the total water depth [3]. As a result of these non-linear shallow-water processes, tidal waves in such regions are often more complex than their linear wave counterparts, with the occurrence of double high or low water, and asymmetries observed in velocity time series due to the presence of overtides. Focussing on the principal semi-diurnal lunar constituent (M_2) and its first overtide (M_4), we can estimate tidal asymmetry from the phase relationship [4]

$$2\emptyset_{M2} - \emptyset_{M4} \quad (1)$$

Methods

We apply the 3D ROMS model to simulate the barotropic currents of the northeast region of Orkney at high resolution ($1/750 \times 1/1451° \sim 75$ m), extending from $3°13.5'$W to $2°25'$W, and from $58°57'$N to $59°16'$N, covering the Westray Firth and Stronsay Firth, which connect *via* the Fall of Warness (the EMEC tidal test site) (inset on Fig. 1). The model was run with 10 vertical (sigma) levels, used the Generic Length Scale (GLS) turbulence scheme, with the coefficients tuned to represent the $k - \varepsilon$ model, and we used a drag coefficient $C_D = 0.003$. Since this is primarily a study of tidal asymmetry, and is not intended as a detailed resource study, we considered only the principal semi-diurnal lunar (M_2) and solar (S_2) constituents. We ran the model for a period of 2 weeks, and validated the M_2 and S_2 components of the vertical tide against data from 6 tide gauges. To validate the horizontal tide, we used ADCP data from the EMEC tidal test site at the Fall of Warness.

Results

We restrict our analysis only to sites where water depth is in the range 25-50 m, and where the peak spring (M_2 and S_2) currents exceed 2 m/s, i.e. locations which are suitable for the majority of first generation tidal stream devices (inset on Fig. 1). These sites are primarily located in Westray Firth and Stronsay Firth. The total area where these depth and velocity criteria are satisfied within the model domain is around 70 km^2 – a substantial region for tidal energy arrays. We selected 21 sites evenly distributed along a 30 km longitudinal transect through Westray Firth and Stronsay Firth, representing a large variability in tidal asymmetry with which to examine its influence on the tidal energy resource.

If we perform tidal analysis on the simulated elevation and velocity time series at each of the 21 selected sites, we can calculate the phase relationship between the M_2 and M_4 constituents, and so calculate the theoretical

* Corresponding author.
Email address: s.p.neill@bangor.ac.uk

asymmetry based on Eq. 1. If we calculate the mean depth-averaged flood velocity over a spring-neap cycle at each location (v_{flood}) and divide by the mean depth-averaged ebb velocity (v_{ebb}), we have a metric for tidal asymmetry (v_{flood}/v_{ebb}) [5]. We plot this value in relation to Eq. 1 and numerical calculations of idealized tidal residuals presented in Neill et al. [6], demonstrating a good fit to the theory (Fig. 1), with a value of $r^2 = 0.81$ (based on analysis of the vertical tide), and $r^2 = 0.69$ (based on analysis of the horizontal tide). There is greater uncertainty when the M_2 and M_4 phase relationship is used to estimate asymmetry from the horizontal tide, since there is much larger spatial variability in the horizontal tide compared to the vertical tide.

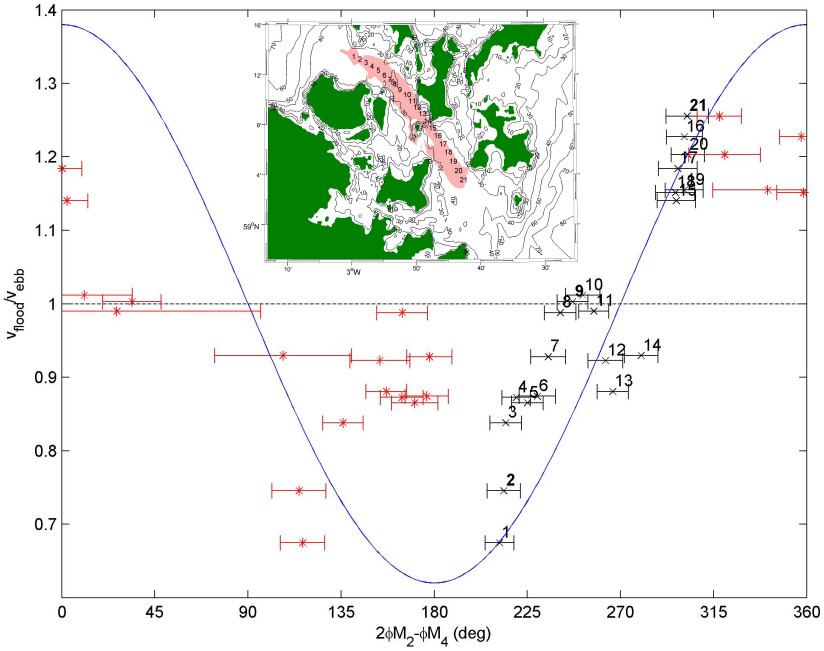

Fig. 1 Modelled tidal asymmetry and theoretical asymmetry, based on Eq. 1 and numerical calculations of idealized tidal residuals presented in Neill et al. [6]. Black crosses=analysis based on the vertical tide; red asterisks=analysis based on the horizontal tide. Error bars indicate 95% confidence intervals estimated by the tidal analysis. Inset shows masked region (light red) and the 21 locations selected for detailed analysis.

Conclusions

At the workshop, we will present results of 3D variables output from the model, including variations of velocity, power and turbulent kinetic energy, and how these variables vary with depth. We also implement the power curve for the SeaGen S 1.2 MW device to explore how tidal asymmetry affects the practical resource, and investigate how tidal asymmetry influences the power extracted at different device hub heights.

Acknowledgements:

This research was funded by EPSRC SuperGen project EP/J010200/1.

References:

[1] Thomson, J., Polagye, B., Durgesh, V., Richmond, M.C. (2012). Measurements of turbulence at two tidal energy sites in Puget Sound, WA. *IEEE J. Ocean Eng.* **37**, 363-374.

[2] Provost, C.L. (1991). Nonlinear tidal interactions in shallow water. In *Generation of overtides and compound tides (review)*, pp. 269-295.

[3] Pugh, D.T. (1987) Tides, surges and mean sea-level. Wiley.

[4] Neill, S.P., Hashemi, M.R., Lewis, M.J. (2014). The role of tidal asymmetry in characterizing the tidal energy resource of Orkney. *Renew. Energy*, **68**, 337-350.

[5] Gooch, S., Thomson, J., Polagye, B., Meggitt, D. (2009). Site characterization for tidal power. In: OCEANS 2009, MTS/IEEE Biloxi-Marine Technology for our future: global and local challenges, pp. 1-10.

[6] Neill, S.P., Litt, E.J., Couch, S.J., Davies, A.G. (2009). The impact of tidal stream turbines on large-scale sediment dynamics. *Renew. Energy* **34**, 2803-2812.

Effects of a tidal farm on the transient and residual circulation of an estuary

Gregorio Iglesias[a*], Marcos Sanchez[b], Victor Ramos[b], Rodrigo Carballo[b], Deborah Greaves[a]
[a]*School of Marine Science and Engineering, Plymouth University, Plymouth PL4 8AA, UK*
[b]*University of Santiago de Compostela, Hydraulic Eng., EPS, 27002 Lugo, Spain*

Summary: This work is concerned with the impact of the extraction of energy from the flow by means of a tidal farm on the transient and residual flow in an estuary. The investigation is conducted through a case study. A 3D, high-resolution hydrodynamics model is implemented and successfully validated based on field data. The model is then applied to investigate the effects of the tidal farm in winter and summer scenarios. After analysing the impacts on the transient flow, the residual flow is considered; it is found that the farm does not alter the two-layer estuarine circulation drastically, but it does weaken the residual velocities over a large area, which could have consequences in terms of water quality and biological productivity.

Introduction

Estuaries are particularly complex and sensitive systems; they are also some of the areas with the largest tidal resource worldwide. Prior to exploiting this resource by means of a tidal stream farm it is fundamental to understand its impacts on the system – with all its complexity. This requires taking into account the effects of the energy extraction not only on the transient circulation (the instantaneous flow velocities) but also on the residual circulation (the net flow over one or a number of tidal cycles). The latter is often disregarded in spite of its importance for water quality and biological productivity, among other aspects.

This work examines the effects of a tidal farm on the 3D transient and residual circulation of an estuary through a case study: Ria de Ortigueira (NW Spain). An estuary of the ria type characterised by a positive estuarine circulation, a pronounced tidal asymmetry in its inner section (with flood dominance) and a high biological productivity, Ria de Ortigueira presents areas with potential for tidal stream exploitation [1].

Methods

The investigation of the impacts of a prospective tidal farm was carried out by means of a 3D hydrodynamics model solving the baroclinic Navier-Stokes equations [2]. The vertical column was discretised into 12 boundary-fitted σ-layers. The horizontal spacing was 50 m × 50 m in the area of interest. The tidal forcing was prescribed through the main nine harmonics (including M4) at the outer grid boundary, and the river inflow was considered with two cases, representative of winter and summer conditions. Using field data from an Acoustic Doppler Current Profiler (ADCP) and a tidal gauge deployed in the inner and middle ria, the model was successfully validated, with values of the correlation coefficients close to unity. The extraction of power from the flow was modelled for the farm using the momentum sink approach. In another investigation into the effects of a tidal farm on the flow in an estuary east of Ria de Ortigueira [3], a high-resolution, 2DH model was implemented, which enabled to represent the extraction of energy by each individual turbine in the farm.

Results

With respect to the transient circulation, it was found that the flow is strengthened by up to 15% (0.3 ms^{-1}) beside the farm, and weakened in front of it and in its lee (Fig. 1). Differences between the winter and summer cases were negligible. The largest impacts occur during the ebb.

As regards the residual flow, its general 3D pattern, and in particular the two-layer, positive circulation in the inner and middle rias, is not altered in any fundamental way by the operation of the tidal farm, but it is weakened by up to 0.03 ms^{-1} (approx. 10-15%); importantly, this reduction in the residual flow extends over a large area (some 2 km away from the farm), much larger than that affected in terms of transient flow

* Corresponding author.
Email address: gregorio.iglesias@plymouth.ac.uk

Conclusions

The consequences of the modifications to the transient and, in particular, residual flow in an estuary caused by a tidal stream farm are far from being fully understood. In light of the previous results, in which it emerged that the residual circulation was affected over a large area, and taking into account the high sensitivity of estuarine systems, it may be concluded that the investigation of the impacts of a tidal farm on the hydrodynamics of an estuary should attend not only to tidal levels or velocities but also to residual flow.

Acknowledgements:

The authors are grateful to the members of the COAST Research Group of Plymouth University and the GICEMA Research Group of the University of Santiago de Compostela for interesting discussions and insight. This research was supported by the grant "Assessment of Renewable Energy Resources" of Spain's Ministry of Science and Innovation.

References:

[1] Iglesias G., Sánchez M., Carballo R., Fernández H. (2012). The TSE index – a new tool for selecting tidal stream sites in depth-limited regions. Renewable Energy **48**, 350–7.

[2] Sanchez, M., Carballo, R., Ramos, V., Iglesias, G. (2014). Tidal stream energy impact on the transient and residual flow in an estuary: a 3D analysis, Applied Energy, **116**, 167-177.

[3] Ramos, V., Carballo, R., Alvarez, M., Sanchez, M., Iglesias, G., 2013. Assessment of the impacts of tidal stream energy through high-resolution numerical modelling, Energy, 61, pp. 541-554.

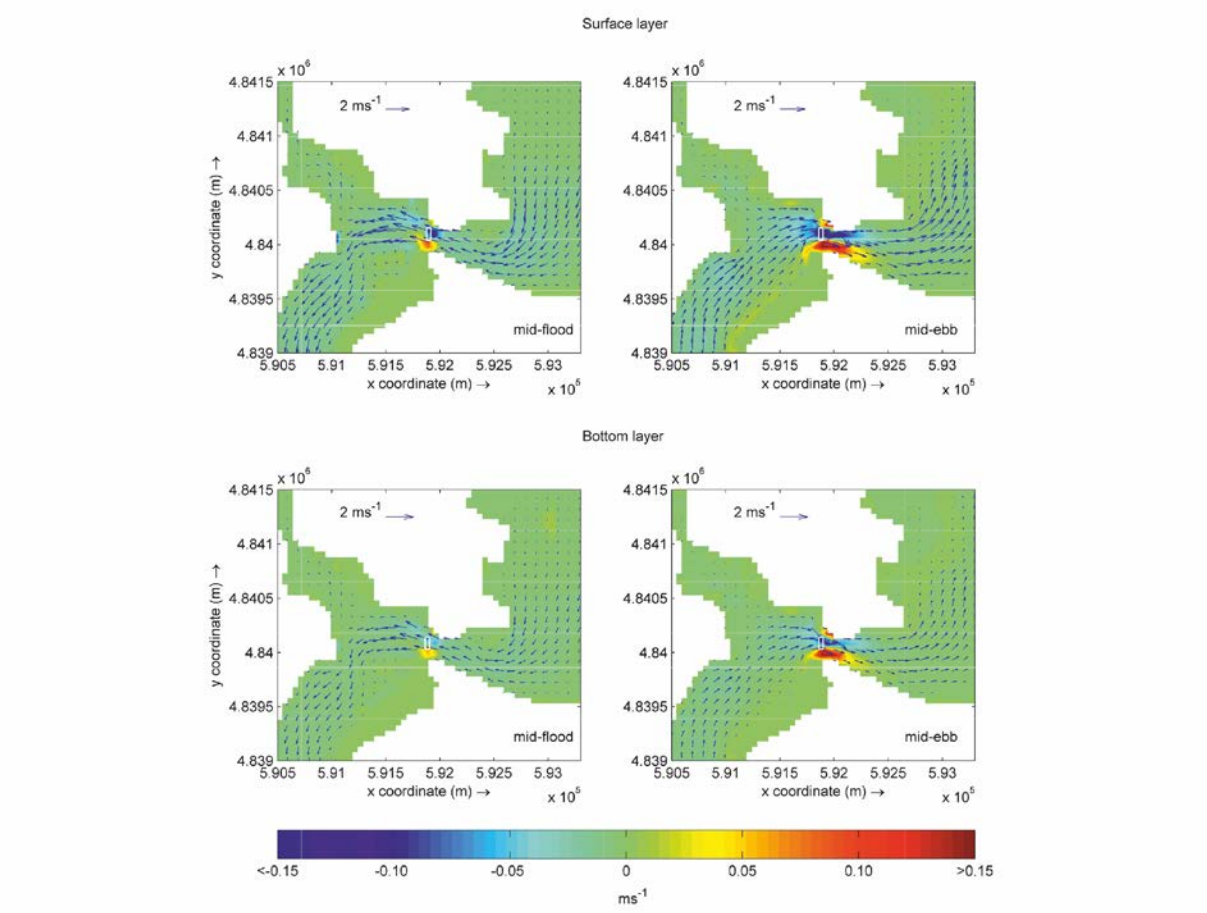

Fig. 1. Modification of the transient circulation caused by the tidal farm in the surface and bottom layers at mid-flood and mid-ebb (winter case).

Impact of support structures on Turbine farm power

Subhash Muchala*, Richard H. J. Willden
Department of Engineering Science, University of Oxford, UK

Summary: The flow characteristics of a channel in the presence of a turbine array are investigated analytically using a 1D model. The impact of support structures on the turbine farm's total power output are not usually considered but we include its influence here and show that it plays a significant role in the power delivered. Also it is shown that installing too many turbines can have a potentially unacceptable adverse effect on the flow rate and the effect of introducing a flow rate reduction constraint is explored.

Introduction

The analytical works of Garrett & Cummins [1], Vennell [2] and Nishino & Willden [3] present various models of flow past turbine arrays but none have extensively considered the impact of support structures. In this paper, we consider the influence of three major factors on the opposing thrust presented to the channel. These components are i. thrust from the turbine rotor, ii. thrust from the support structure and iii. seabed friction. The influence of these factors on various output parameters such as the efficiency of the turbine, number of turbines that can be installed in a channel, total power output from the farm and power output per turbine are studied. These parameters are studied for different channel characteristics.

Method

We consider a channel of rectangular cross section, A_c, length $L = 5\text{km}$, width, $w = 1\text{km}$ and depth, $h = 40\text{m}$. The 1D Euler equation for flow in the channel is given by

$$\frac{\partial u}{\partial t} + u\frac{\partial u}{\partial x} + g\frac{\partial \xi}{\partial x} = -F \tag{1}$$

where u is the flow velocity, ξ and F are the driving head and resistive force per unit mass respectively. Following Garrett & Cummins [1], we write the flow velocity in terms of volume flow rate ($Q = A_c u$) and integrate equation (1) along the channel. We assume that the flow is drawn into and exits the channel smoothly. Representing the driving head as a sinusoidal tide with amplitude a and frequency ω, we obtain

$$c\frac{dQ}{dt} - ga\cos(\omega t) = -FL \tag{2}$$

where c is the area coefficient given by $\int_0^L A_c^{-1}\,dx$.

The total opposing force in the channel is given by

$$F = \frac{1}{\rho L A_c}\frac{1}{2}\rho u|u|\left[n\left(C_T A_t + C_D A_s\right) + C_f A_b\right] \tag{3}$$

where n represents the number of turbines installed in the channel; C_T, C_D, C_f are the coefficients of turbine thrust, support structure drag and seabed friction; A_t, A_s, A_b are the turbine rotor area, support structure frontal area and channel bed area. The first two terms on the right hand side are due to the presence of turbines and their support structures respectively and the third term is due to seabed friction. The volume flow rate (or velocity) is clearly a function of the opposing force and solution of (2) and (3) is achieved through time marching.

Results

We consider a realistic turbine with a rated power of 1MW achieved at a flow speed of 2.5m/s ; see Fig. 1(a). We consider a range of support structure drag coefficients $0 \le C_D \le 1.8$ for the ratio, $\chi = A_s / A_t = 0.2$, resulting in total (rotor and support structure) turbine thrust as shown in the figure. We observe that the efficiency (ratio of power generated to power removed from the flow) of a turbine drops due to its support structure and that this drop is greatest for higher velocities; see Fig. 1(b).

* Corresponding author. *Email address*: subhash.muchala@eng.ox.ac.uk

From solution of equations (2) and (3), the volume flow rate, power and thrust curves are plotted for one tidal cycle; see Fig. 2(a). The two thrust curves represent the rotor thrust and total turbine thrust; rotor and support structure. The rotor thrust reaches its peak before and after the peak flow rate due to feathering once rated power has been reached. We can observe that the volume flow rate remains almost sinusoidal whereas the power curve exhibits a capped behaviour due to the rated power constraint.

The power output from the turbine farm has been studied for different numbers of turbines installed in the channel and plotted against the total opposing thrust in the channel; see Fig. 2(b). It is observed that the support structure drag has a significant influence on the total farm power that can be delivered by the turbines. We further explore the reduction in flow rate required to achieve given levels of power yield and observe that even large permissible reductions in flow rate, say 10%, together with realistic values of support structure drag, $C_D = 1.2$, lead to very significant reductions in available power below what might be hypothesized for unconstrained energy extraction.

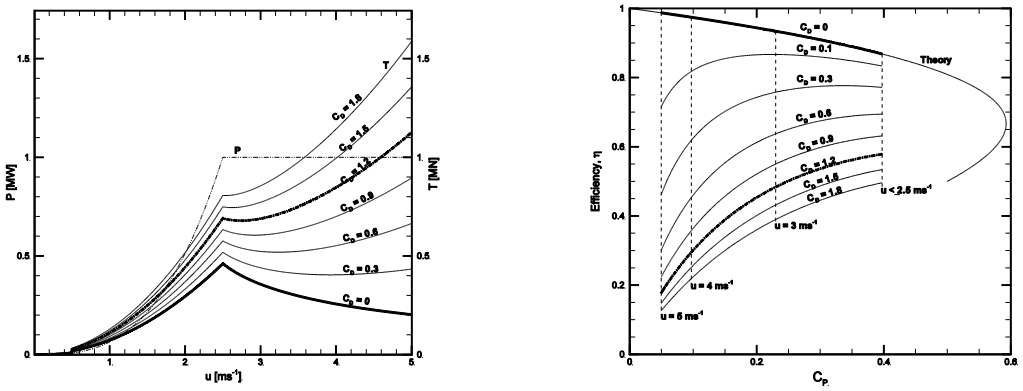

(a) (b)

Fig. 1. (a) Power-Thrust and (b) efficiency curves of a turbine for different support structure drag coefficients.

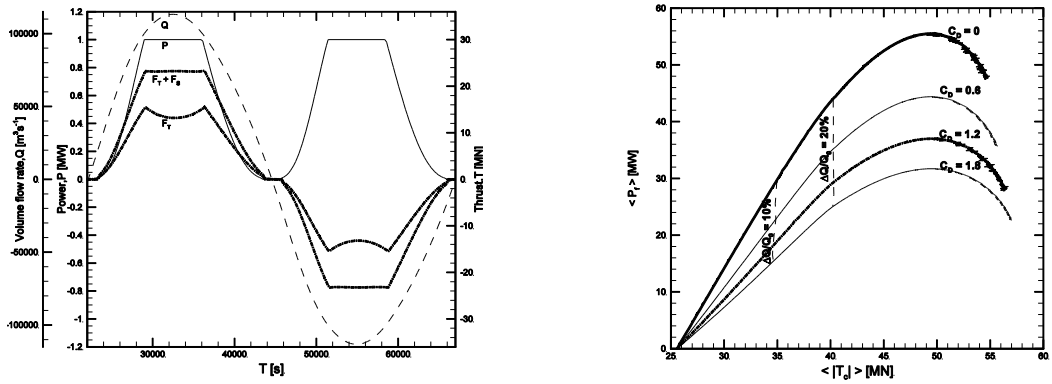

(a) (b)

Fig. 2. (a) Flow rate, turbine thrust and power variation over the tidal cycle, (b) time average farm power as a function of farm thrust for various levels of support structure drag; $C_f = 0.002,\ \omega L/\sqrt{ag} = 0.478,\ L/h = 125,\ \chi = 0.2.$

Conclusions

It has been observed that an increase in the support structure drag coefficient leads to a decrease in the efficiency of the turbine and also the power output from the turbine farm. And that flow rate reduction constraints act to further reduce the power that can be developed by a tidal farm. Hence structures with low drag coefficients should be used for the support structures of tidal turbines.

References:

[1] Garrett, C. & Cummins, P. (2005). The power potential of tidal currents in channels. *Proc. R. Soc. A* **461**.
[2] Vennell, R. (2012). The energetics of large tidal turbine arrays. *Renew. Energy* **48**.
[3] Nishino, T. & Willden, R. H. J. (2013). Two-scale dynamics of flow past a partial cross-stream array of tidal turbines. *J. Fluid Mech.* **730**.

Assessing the Hydro-Environmental Impacts of Tidal Turbines

Anna Phoenix
Department of Engineering, National University of Ireland, Galway
a.phoenix2@nuigalway.ie

Summary: Tidal stream turbines have the ability to supply a sizeable proportion of the world's energy demands. The hydro-environmental impacts associated with tidal turbine deployment can include both near field effects in the waters immediately adjacent to the turbines and far field effects such as alteration to the estuary-wide tidal regime. These effects are, as yet, still relatively unknown although numerical models have been used to show that they can be significant. This research aims to develop a methodology that can be used to determine the maximum energy that can be extracted from a tidal water body without significant adverse environmental impacts.

Introduction

Tidal current turbines have the potential to provide a considerable proportion of global energy requirements. At present the commercial viability of marine current devices is being tested using single devices; however investigation into large-scale tidal turbine arrays has yet to be significantly explored. The feasibility of such technology will depend on the expected power output, as well as the consequential hydro-environmental impacts.

This research aims to determine a methodology to quantify and assess the significance of these impacts. A resulting significant impact factor will be developed that reflects the fraction of kinetic energy that can be extracted using tidal turbine devices without significant environmental effects. A second long term goal will be to develop an approach using flushing to identify the array layout that would achieve maximum energy output whilst minimising adverse environmental impacts.

Methods

The methodology will primarily involve numerical modelling. The model system is a two-dimensional finite difference model. The source code of the model will be assessed and modified to include a flushing analysis capability.

Basic statistical and data analysis techniques, such as regression analysis, will be used to analyse model output so that the hydrodynamic and environmental impacts may be quantified and relationships between impacts and power extraction can be formulated.

Physical modelling techniques will be used to construct scale models in a tidal basin and perform measurements and observations of current speeds, water levels and solute transport. These measured data will be used to validate the numerical model.

The developed model will be applied to idealised cases to assess the impacts due to various turbine array layouts. The model will also be applied to a case study site, namely, The Shannon Estuary.

Additionally a detailed review of relevant literature and research to date will be carried out. The focus will be on reviewing and comparing both experimental tests and numerical modelling studies into assessing the associated impacts of tidal turbines.

Results

Recent research has identified the main hydrodynamic impacts associated with tidal turbine deployment as changes to water surface elevations and current velocities. Studies show that impacts on the tidal range will be minimal, however changes to current velocities have the potential to be significant.

Whilst the extent of these influences will be site specific, in general it has been found that tidal stream energy extraction will result in a velocity deficit immediately upstream and downstream of the turbines as well as inside an array. The velocity deficit exists up to a considerable distance downstream of a turbine, but will gradually recover, returning to free stream velocity as flow moves further away from the device. This is illustrated in the velocity deficit profiles presented in Figures 1 and 2 below.

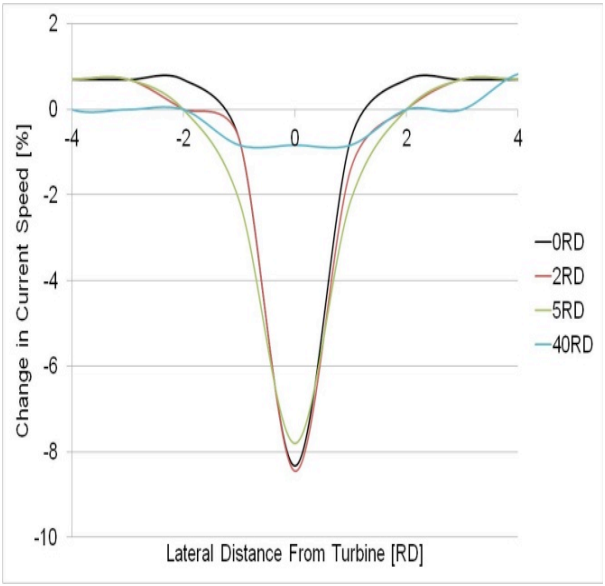

Figure 1:Velocity deficits along lateral transects at various distances downstream of a turbine [1]

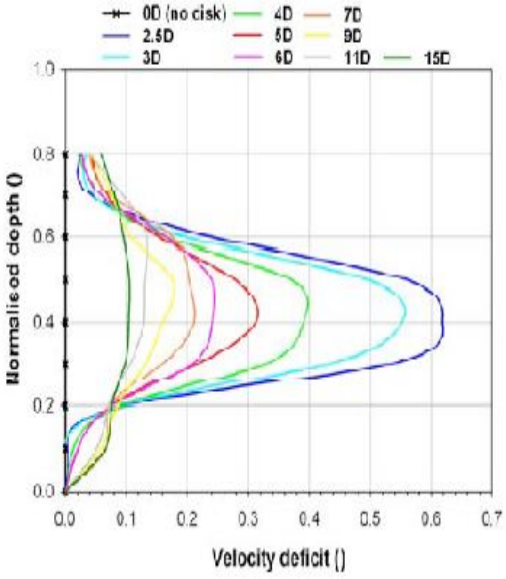

Figure 2:Vertical velocity deficit profiles downstream of a porous disc [2]

These alterations to the tidal regime will have associated environmental impacts, such as changes to sedimentation rates and other costal processes including bacterial and pollutant concentrations in the water column, and may also have negative implications for marine life.

If commercial tidal turbine deployment is to be achieved the significance of these impacts will have to be constrained to a point at which adverse environmental effects do not occur. Published studies have established initial guidelines for a significant impact factor, which is defined as the percentage of the total kinetic energy resource at a site that could be extracted without significant economic or environmental effects [3]. Based on this it is proposed to develop an impact index, using flushing time as the environmental indicator, which would indicate the significance of hydro-environmental impacts for different turbine arrays. Such a tool would be of enormous benefit in the planning and siting of tidal turbine arrays.

Conclusions

Research to date has demonstrated that the hydro-environmental impacts associated with tidal turbine deployment may be substantial and adverse, having the potential to change the underlying hydraulic characteristics of tidal environments.

If large-scale turbine deployment is to be deemed environmentally viable the tidal kinetic energy extracted at a site will have to be limited, at present this constraint is estimated to be 20% [4].

Tidal stream turbine technology is still in its infancy and further research into this area is required. The proposed numerical modelling will enable a more detailed assessment into quantifying the significance of the associated impacts of tidal turbine deployment, allowing accuracy of the significant impact factor to be increased. Once this is achieved a design for an optimum array layout with maximum energy extraction and minimal adverse hydro-environmental impacts can be determined.

References:

[1] Nash, S, et al. (2013). *Investigating the Optimal Layout of a Tidal Turbine Array using Numerical Modelling*.

[2] Bahaj, A.S, et al. (2007). *Characterising the Wake of Horizontal Marine Current Turbines.*

[3-4] Black and Veatch (2005) *Phase 2, UK Tidal Stream Energy Resource Assessment.*

Effects of Dynamic Inflow and Distortion of Incident Turbulence on Tidal Turbine Rotors.

Duncan M. McNae, J. Michael R. Graham
Department of Aeronautics, Imperial College London, UK

Summary: This paper describes numerical simulation using a vortex panel free wake model and water flume experiments to evaluate added mass and dynamic inflow for unsteady flow through a horizontal axis tidal stream rotor. The reason for the much smaller inflow effect caused by changes in incident axial flow in comparison with matched amplitude and frequency changes in blade pitch is discussed. The second part of the paper analyses turbulence in the incident flow by the rotor mean flow field as it approaches the rotor plane.

Numerical simulation of unsteady flow.

The flow through a twin bladed horizontal axis tidal stream turbine has been computed using a numerical potential flow method in which the blade camber surfaces are replaced by doublet panels (or equivalently a vortex lattice) with the Kutta-Joukowski condition satisfied at the trailing edge. Vorticity is shed into the rotor wake in the form of line vortex elements which are convected as a free wake by the local velocity field. This allows the vortex wake to roll up and become displaced from the uniform helical geometry of a 'frozen' wake, as is shown in figure 1. Forces on the rotor blades are computed using the unsteady Bernoulli equation for pressures following a modified form of the method described in [1]. This is found to give the most accurate treatment of the in-plane force associated with the pressures around the leading edge of a thin blade which are singular in this lifting-surface approximation. The numerical method was used to compute the out-of-plane blade root bending moment in unsteady flow and the axial force on the rotor.

Measurements on a model rotor in unsteady flow.

Experimental measurements were also carried out on an instrumented model rotor in a water flume of width 0.6m with the rotor located at mid-depth in a water flow 0.7m deep. The model rotor was 0.4m in diameter (and hence operating under high blockage conditions) with two blades of NACA6412 section. It rotated about a horizontal axis, mounted on a single thin, vertical support strut of approximately 0.03m diameter more than 5 diameters behind the rotor to eliminate tower shadow. The strut was strain-gauged to provide measurements of the axial force induced on the rotor. The blades, one of which was strain-gauged for out-of-plane bending moment at its root, were attached to an instrumented hub equipped with radio transmission of the bending moment signal to a fixed antenna in the rotor nacelle. The nacelle also contained an electromagnetic brake to provide constant torque rotor speed control. Further details are given in [2]. Apart from some measurements to help validate the numerical predictions the study focused on effects of unsteady uniform incident flow on the rotor loading as a simplification of unsteady flows associated with either incident flow turbulence or wave action from the surface. Oscillatory relative incident flow was generated by supporting the rotor from a computer controlled carriage above the flume which followed a sinusoidal motion, oscillating the rotor streamwise in a mean flow of 3% turbulence intensity and 5% mean flow variation. Measurements of axial force on the rotor and blade root bending moment were taken and compared with the numerical simulations for the same relative velocities (or current numbers) and these comparisons will be discussed.

Effects of dynamic inflow.

The numerical code was used to examine the effects of impulsive changes in incident velocity and correspondingly impulsive changes in blade pitch. These step changes were scaled to give asymptotic long-time matched conditions of axial force or induction velocity. Rapid changes in pitch are known to generate considerable overshoot in force due to the strong effect of dynamic inflow (lag of wake induced velocity) but a much smaller overshoot is observed for impulsive changes in incident velocity. A typical comparison from the present simulations is shown in figure 2. The reason for the difference can be understood from the wake induced velocity fields which have been extracted separately from the whole velocity field in the numerical simulations, and will be discussed.

Distortion of incident turbulence.

Because both surface wave effects and turbulence in the tidal stream are of a scale which is not very large compared with the scale of the rotor (or for multi-turbine deployments the array) both incident fields are distorted by the resistance of the rotor. Wave diffraction has been extensively studied for large marine structures. Less extensively distortion of turbulence by the mean velocity strain field of a body has been analysed by rapid distortion theory (RDT). Homogeneous distortion as in wind-tunnel contraction flow was analysed in [3] and non-homogeneous distortion by the flow field of a bluff body in [4]. Effects of weak non-homogeneous strain due to flow through a porous plate were investigated in [5]. All demonstrated significant effects of distortion on turbulence length scales smaller than the length scale of the body. Tidal stream turbines generate a flow field similar in the mean to a porous disc and therefore similar distortion effects may be expected. Detailed computation of non-homogeneous distortion involves numerical evaluation of many multiple integrals over the flow field, is computationally very expensive and not practical. Actuator disc theory approximates rotor flow 1-dimensionally and allows homogeneous strain analysis to be a good approximation for smaller length scales. Being the opposite of a contracting flow the mean strain increases the axial velocity component in the turbulence while decreasing the cross-stream components. This effect increases significantly the amplitude of unsteady tidal turbine rotor loading as discussed in [6], 1-dimensional RDT results for a horizontal axis rotor being presented in [7]. The present work presents similar analysis indicating increases of order 20% on loading and will be discussed together with a further development of the analysis for the frequency spectrum of the distorted flow.

Summary of Conclusions.

Numerical simulation supported by experimental code validation has demonstrated and analysed the much smaller effects of dynamic inflow due to rapid change in flow velocity compared with rapid blade pitch change. Theoretical analysis has indicated that the effects of rapid distortion of incident turbulence by the mean flow field of the rotor can significantly increase the streamwise velocity fluctuations at the rotor particularly at low frequency.

References:

[1] Katz, J. and Plotkin, A. (1991). *Low Speed Aerodynamics*, McGraw-Hill.
[2] McNae, D. M. (2014). Unsteady Hydrodynamics of Tidal Stream Turbines. *PhD Thesis, Imperial College London.*
[3] Batchelor, G. K. and Proudman, I. (1954). The effect of rapid distortion of a fluid in turbulent motion. *Q. J. Mech. Appl. Maths , Vol. 7, 83-103*.
[4] Hunt, J. C. R. (1973). A theory of turbulent flow round two-dimensional bluff bodies. *J. Fluid Mech., Vol. 61, 625-706*.
[5] Graham, J. M. R. (1976), Turbulent flow past a porous plate. *J. Fluid Mech., Vol. 73, 565-591*.
[6] Milne, I., (2014), *PhD Thesis, University of Auckland.*
[7] Farr T.D. and Hancock, P.E., (2013), Torque fluctuations caused by upstream mean flow and turbulence. *Internal report to SuperGen Wind II (EPSRC) Consortium.*

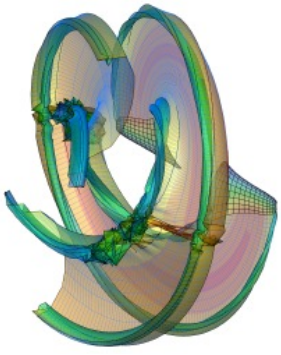

Figure 1 Rotor Wake.

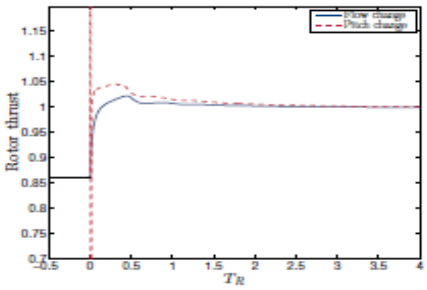

Figure 2. Rotor axial force due to impulsive pitch and velocity changes. (TSR = 4.0 at T_R = 0.0, $\Delta\alpha = 2^o$, ΔU = 8%.)

The Effect of Tidal Flow Directionality on Tidal Turbine Performance Characteristics

Carwyn Frost*, Ceri Morris, Allan Mason-Jones, Daphne O'Doherty, Tim O'Doherty
Cardiff Marine Energy Research Group, School of Engineering, Cardiff University

Summary: As marine turbine technology verges on the realm of economic viability the question of how long will these devices last is an important one. This paper looks at the axial bending moments experienced from CFD modelling of Cardiff University's concept tidal turbine in a uniform profile for three different scenarios. The magnitude and direction in which the axial bending moment acts is an important feature in determining likely sources of wear in the drive train, such as bearings. By determining the source and magnitude of these bending moments, possibilities for reducing them and limiting their impact on devices can be made.

Introduction

As full scale prototypes are begin tested and meeting the challenges of the marine environment there are various design philosophies still being trialled with some sign of convergence on a generic design as has been seen in the wind sector. The primary focus of designers has been into HATTs. Many of these devices are supported by a cylindrical support tower or stanchion, however little work has been published on the direct effect of such a support structure on the axial bending moments of a HATT, especially when the stanchion is upstream of the blades, as could be the case for turbines operating in bi-directional tidal flow. The basis of this work comes from prior work by Mason-Jones et al [1] which found the presence of asymmetric loading on turbines and the compounded complexity with the presence of a stanchion. Using the same turbine and similar cylindrical stanchion the work in this paper focuses on the magnitude and direction of the resultant axial bending moments acting on the drive shaft from the turbine. Three scenarios are considered; a) with no stanchion, b) turbine in front of the stanchion and c) turbine behind the stanchion. Validation has been established through a comparison of the Power Coefficients between the no stanchion case with the previous study [1], though on going experimental work in progress.

Methods

ANSYS CFX is a Computational Fluid Dynamics (CFD) modelling package which offers well documented and validated success in its field. For the models being considered the Reynolds Averaged Navier Stokes (RANS) equations were used along with the Shear Stress Transport (SST) equation as the viscous model to close the equations. To determine the axial bending moments acting on the shaft during a single rotation a transient CFD model was used. During operation, axial thrust loads act at the centre of pressure on each of the turbine blades. These give rise to bending moments which can be measured about the vertical and horizontal axis (M_X and M_Y).From this, the magnitude of the resultant axial bending moment is obtained and the angle at which it is acting.

It is expected that the angle of bending moment will align itself toward the dominant bending moment either about the x or y axis. If the moment in the x-direction is greater than the moment in the y-direction the angle of bending moment is expected to be close to 90° or 270°. Likewise if the moment in the y-direction is greater than that in the x-direction the angle will be closer to 0° or 180°.

Results

a) No Stanchion

When there is no stanchion present the resultant bending moment from the turbine about the rotating axis is small but present as can be seen from Figure 1. There are three peaks/ troughs in the data which suggests a slight inherent bending moment, this may come from the geometry of the blades however its magnitude is such that it is negligible in comparison to when there is a stanchion present.

b) Turbine in Front of the Stanchion

Figure 2 shows non-symmetric axial loading is exerted on the drive shaft, resulting in an axial bending moment. There are 6 distinct peaks and troughs in the magnitude of the bending moment during one rotation. The peaks correspond with when one of the blades has just passed the stanchion at either Top Dead Centre (TDC) or Bottom Dead Centre (BDC). This suggests there is a delayed interaction between the blades and stanchion. As the flow diverges around the stanchion the passing blade will experience significantly lower axial thrust than the other two blades in the unsheltered flow, thus the axial bending moment increases. As the blade moves out from the sheltered area in front of the stanchion its axial thrust increases, evening the distribution and reducing the axial bending moment. The angle of the bending moment follows the rule stated in above section. The curve is a repeating pattern every 120°, considering this first cycle in Figure 2, the angle is continually decreasing showing the direction of the bending moment is moving in an anti-clockwise manner. However there are 2 distinct interruptions in the gradient of this slope and these correspond to the peaks of the axial bending moment when one blade has just passed though TDC or BDC.

c) Turbine Behind the Stanchion

Figure 3 shows significant non-symmetric loading being exerted on the drive shaft. This results in much greater axial bending moment. Again there are 6 distinct peaks and troughs in the magnitude of the bending moment during one

* Corresponding author.
Email address: FrostC1@Cardiff.ac.uk

rotation. The increased amplitude between peak and trough is due to the increased shelter the blade passing the stanchion receives. Being in the wake of the stanchion the axial thrust on the blade is significantly less, however the blades in unsheltered flow experience the same axial loads as before. The increased difference between the axial loads on the blades leads to the increased axial bending moment. Notice the magnitude of the troughs has not changed between the two stanchion cases. This is because when all blades are equally exposed in both scenarios (b & c) the axial thrusts on them have the same even distribution. The location of the peaks and troughs has shifted due to the flow having to pass the stanchion before interacting with the turbine. The angle or direction of bending moment has also been affected by this. In the previous case the angle showed an anticlockwise (decreasing) pattern. In this circumstance there is a clockwise (increasing) pattern. The rule relating to the dominant bending moment and direction remains true, and again there are two distinct interruptions in the gradient of the curve which correspond with the blades entering the shadow of the stanchion.

Conclusions

The presence of such significant axial bending moments, as seen in scenario c) is undesirable due to its inevitable impact on the wear of drive train parts. Bearings along the drive shaft of the turbine will suffer significant fatigue issues from such loading regimes, resulting in shorter maintenance periods and increasing the cost per kWh on the turbine.
It has been established that the source of the significant axial bending moments comes from the interaction with the stanchion. As is clear removing the stanchion would be the best solution; however that is not possible with many designs. Therefore the reduction of these axial bending moments must be made; the use of a yaw mechanism would maintain the turbine upstream of the stanchion, preventing the more severe scenario. In addition, reducing the stanchions diameter or replacing with a hydrodynamic profile would also reduce these moments.
This work is limited to the effect of the stanchion on these bending moments. Other issues must also be considered for a true system such as velocity profiles [1] and waves [2].

Acknowledgements:

We would like to thank, Mabey Bridge, HPC Wales and UKCMERG for their support.

References:

[1] Mason-Jones A, O'Doherty DM, Morris CE, O'Doherty T. (2013) *Influence of a velocity profile & support structure on tidal stream turbine performance.* Renewable Energy 52 (2013) 23-30

[2] McCann GN. (2007) *Tidal current turbine fatigue loading sensitivity to waves and turbulence – a parametric study.* 7th EWTEC

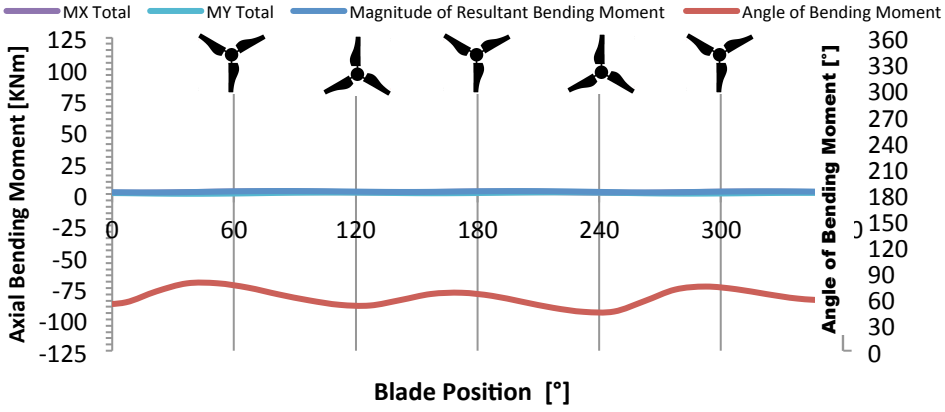

Figure 1 Axial Bending Moment over a rotational cycle of the turbine a) No Stanchion

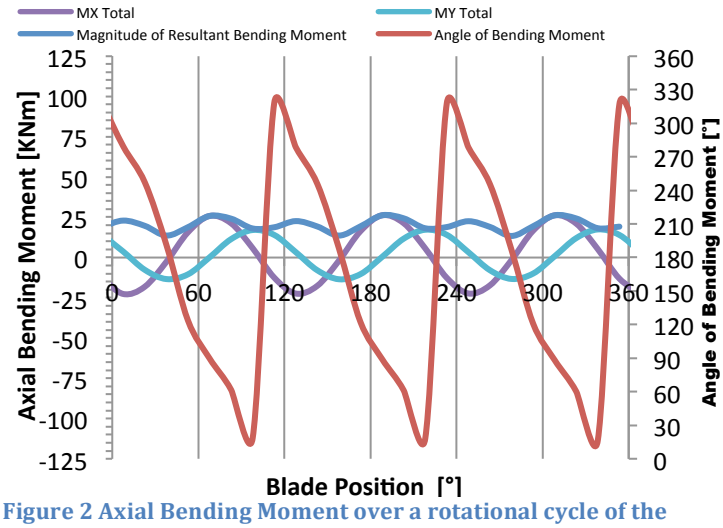

Figure 2 Axial Bending Moment over a rotational cycle of the turbine. b) Turbine in Front of the Stanchion

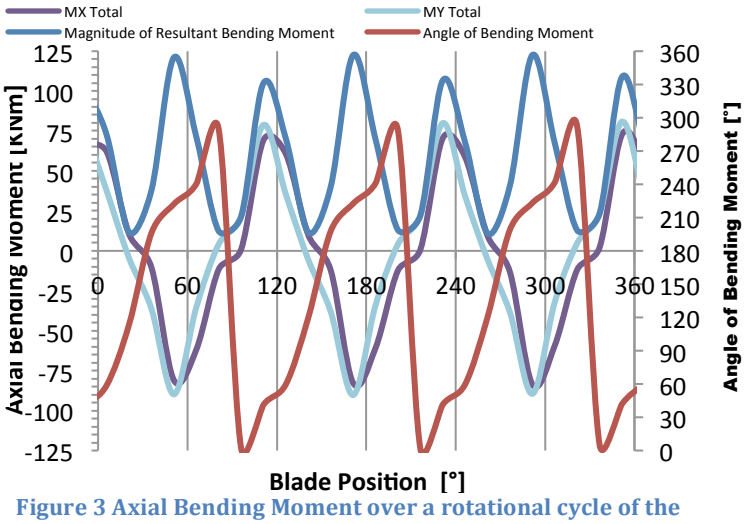

Figure 3 Axial Bending Moment over a rotational cycle of the turbine. c) Turbine in Behind the Stanchion

Modelling Pressure Changes in the Vicinity of Tidal Turbines to Assess Fish Survival Rate During Turbine Passage

Enayatollah Zangiabadi*, Ian Masters, Alison J. Williams, T.N. Croft
College of Engineering, Swansea University, SA2 8PP, UK

Allan Mason Jones
School of Engineering, Cardiff University, CF24 3AA, UK

Summary: Estuaries and channels, which are potential deployment sites for Tidal Stream Turbines (TST), are home to many marine mammals and fish species. One issue that has to be considered before the installation of TSTs is the interaction of these devices with the resident fauna. The pressure change, cavitation and turbulence are among the main factors that endanger the animal during passage through the turbine [1]. In this article, by using BEM-CFD and blade resolved CFD methods, the survival rate for fish is investigated for single and multiple tidal turbine arrays. The results show that if a fish passes through the swept area of the turbine, the majority of the species are able to survive the incident.

Introduction

Apart from the risk of being hit by the blades of the turbine, the other major threat for the fish is the rapid pressure change as it passes through the disk that describes swept area of the turbine. There is a pressure increase in front of the turbine which is followed by a sudden pressure drop immediately behind the turbine. Then the pressure gradually increases again to ambient pressure. For most fish, the main cause of mortality is the damage caused to the internal organs, in particular to the swimbladder. The drastic change in the volume of the swimbladder due to the almost instantaneous pressure change is the main reason for fish mortality[2]. Less significant are the cavitation and turbulence imposed into the water by the TST.

Simulations have been performed for a single device and triangular array configuration using the steady state k-ε turbulence method. The results are then compared with experimental data which were available mainly for the survival of fish going through hydroelectric dams.

Methods

Two different approaches have been used to simulate the fluid flow around a tidal stream turbine. The first approach, which has a shorter run time, uses the Blade Element Momentum Theory coupled with Computational Fluid Dynamics (BEM-CFD) method. In this method the turbine effects are time averaged over a long period of time so that the influence of the blades varies according to radial position based on the property of the blades (chord, twist, etc.) at the given location. [3]. The second takes into account the full turbine Blade Resolved Geometry (BRG) and uses a transient CFD model, resulting in significantly longer run times.

Pressure values are measured along stream traces which are the likely swimming path for the fish. Based on the maximum and minimum values of the pressure, the high risk and low risk location along the swimming path relative to the turbine were identified.

In order to have a direct comparison between the two models, a standard finite volume approach with a k-ε turbulence model has been employed to conduct both simulations. The BRG model, including the Finite Volume model construction and set up, was provided by the Marine Energy Research Group of Cardiff University. It has a 10 m diameter turbine in a rectangular domain with the dimension of $506 \times 50 \times 50$ meters in which the turbine is located 104 meters from the inlet. The inlet boundary conditions are defined as a uniform flow in which the flow speed is 3.086 m/s and the bed has a non-slip wall condition. To run the simulation, the rotational speed of the blade is set to 2.25 rad/s which is the optimum rotational speed for the rotor in normal operation. The zone that represents the rotation of the rotor, has a 17 m diameter and 6 m width. The BEM-CFD model for the single array turbine has exactly the same dimensions and boundary conditions.

For the triangular array the computational domain consists of a rectangular channel with 700 m length, 200 m width and 30 m depth. The turbines are positioned so that the centres are at the midpoint of the channel depth, with the first row of turbines located 300 m from the inlet. The configuration has two turbines in the first row which are 15 m apart. The second row turbine is located 75 m downstream at a lateral position that is midway between the first row turbines to form a triangular shape TST array.

* Corresponding author:
Email address: 502830@swansea.ac.uk

Results

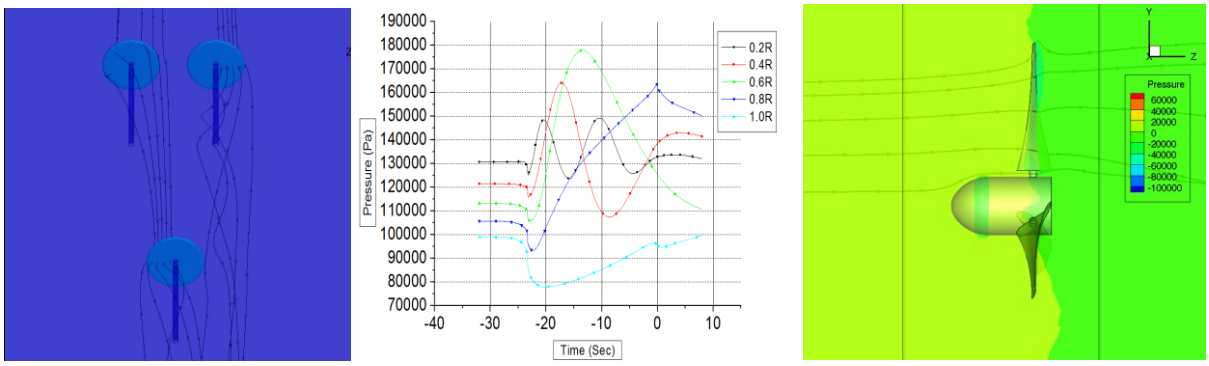

Fig. 1. Stream lines along the length of the channel and through the turbines (left); Pressure Change along the Vertical Section Perpendicular to the Hub of a Tidal Turbine for the First and Second Row of Turbines in the Triangular Configuration for a Tidal Array (middle); Stream lines passing adjacent to the blades of a 10m diameter rotor (right)

The computational results are compared with some existing data:

Radius	**0.2R**	**0.4R**	**0.6R**	**0.8R**	**1.0R**
Pressure Change (kPa)	4.4	4.1	4.4	4.7	3.5

Table 1 Pressure Change along the Length of the Blade for a 5m Radius Turbine in the First Row of a Triangular Configuration Tidal Array

Species	Death	Injury
Bluegill Sunfish	~51 kPa	>51 kPa
Fall Chinook Salmon	91-99 kPa	91-99 kPa
Rainbow Trout	91-99 kPa	91-99 kPa

Table 2 amount of Pressure values at which mortality/injury occurs for three species [2]

Conclusions

It is clear that the amount of the pressure change that the fish encounter during swimming through a tidal turbine does not significantly endanger the life of the species. There are some locations where the pressure gradient is large but as those zones are located very close to the leading edge of the turbine, the fish going through those areas are likely to be damaged by the impact force from the blade rather than the pressure change. Studies on the interaction of fish and hydroelectric dams [1] showed that the main issue is the head difference before and after the turbine which this is not the case in the TSTs. The effect of cavitation and turbulence require further study, but appear to be negligible. Cavitation happens very close to the blade and turbulence causes some disorientation for the fish.

Acknowledgements:

The Authors wish to acknowledge the financial support of the Crown Estate, Welsh Assembly Government, the Higher Education Funding Council for Wales, the Welsh European Funding Office, and the European Regional Development Fund Convergence Programme.

References:

1. Cada, G.F., *Shaken, Not Stirred: The Recipe for a Fish-Friendly Turbine*, E.S. Division, Editor. 1997, Oak Ridge National Laboratory: Oak Ridge.
2. Becker, J.M., C.S. Abernethy, and D.D. Double, *Identifying the Effects on Fish of Changes in Water pressure during Turbine Passage*, in *Hydro Reveiw*. 2003, HCI.
3. Malki, R., et al. *A Numerical Investigation into Tidal Stream Turbine Wake nDynamics and Device Performance in Non-Uniform Flow* in *International Offshore and Polar Engineering Conference* 2012. Rhodes, Greece: International Sciety of Offshore and Polar Engineering.

OTE 2014 - Participants

McNaughton, James	Alstom Ocean Energy
Vigars, Paul	Alstom Ocean Energy
Paillard, Benoit	Alternative Current Energy
Neill, Simon	Bangor University
Cohen, Claire	Black & Veatch
Frost, Carwyn	Cardiff University
Mason-Jones, Allan	Cardiff University
O'Doherty, Daphne	Cardiff University
Camosi, Luca	Cranfield University
Farman, Judith	Cranfield University
Gunn, Kester	E.ON
Stock-Williams, Clym	E.ON
Abolghasemi, Mohammad	Imperial College London
Culley, David	Imperial College London
Graham, Michael	Imperial College London
Cliquet, Vincent	Innosea
Quayle, Stephen	Lancaster University
Phoenix, Anna	National University of Ireland, Galway
Chapman, Simon	North Sea Systems
Morgan, Mungo	North Sea Systems
Iglesias, Gregorio	Plymouth University
Chatzirodou, Antonia	Swansea University
Edmunds, Matt	Swansea University
Lake, Thomas	Swansea University
Masters, Ian	Swansea University
Togneri, Michael	Swansea University
Zangiabadi, Enayatollah	Swansea University
Carlier, Clément	Université du Havre
Pinon, Grégory	Université du Havre
Buldakov, Eugeny	University College London
Simons, Richard	University College London
Sequeira, Carl	University of Cambridge
Haverson, David	University of Edinburgh
Pérez-Ortiz, Alberto	University of Edinburgh
Bruce, Esther	University of Hull
Olczak, Alex	University of Manchester
Stallard, Tim	University of Manchester
Adcock, Thomas	University of Oxford
Byrne, Byron	University of Oxford
Cooke, Susannah	University of Oxford
Fleming, Conor	University of Oxford
Hunter, William	University of Oxford
McAdam, Ross	University of Oxford
Muchala, Subhash	University of Oxford
Nishino, Takafumi	University of Oxford
Payo, Andres	University of Oxford
Serhadlioglu, Sena	University of Oxford
Vogel, Christopher	University of Oxford
Willden, Richard	University of Oxford
Kirke, Brian	University of South Australia
Wimshurst, Aidan	University of Southampton
Nevalainen, Thomas	University of Strathclyde
Cavagnaro, Robert	University of Washington
Draper, Scott	University of Western Australia
Campbell, Thomas	(individual participant)